공학석사 학위논문

Development of Three-ring Conductance Sensor Based on FPCB for Measuring Liquid Film Thickness under Non-isothermal Condition

비등온조건의 액막두께 측정을 위한 연성회로기판 기반 3-전극 센서 개발

2016년 2월

서울대학교 대학원

에너지시스템공학부

이 규 병

Development of Three-ring Conductance Sensor Based on FPCB for Measuring Liquid Film Thickness under Non-isothermal Condition

비등온조건의 액막두께 측정을 위한 연성회로기판 기반 3-전극 센서 개발

지도교수 조 형 규

이 논문을 공학석사 학위논문으로 제출함

2016년 2월

서울대학교 대학원
에너지시스템공학부
이 규 병

이규병의 석사학위 논문을 인준함

2016년 2월

위 원 장 김 응 수 (인)
부위원장 조 형 규 (인)
위 원 어 동 진 (인)

Abstract

Development of Three-ring Conductance Sensor Based on FPCB for Measuring Liquid Film Thickness under Non-isothermal Condition

Kyu-Byoung Lee
Department of Nuclear Engineering
The Graduate School
Seoul National University

Liquid film thickness is an important factor in understanding the two-phase annular or film flow. Thus, a lot of researches have been conducted in order to measure the local liquid film thickness. Generally, measuring the liquid film thickness with high time and spatial resolution has been limited in two-phase flow experiments. Recently, simultaneous measurement of the local liquid film thickness with high time and spatial resolution have become possible by coupling electrical conductance method with wire-mesh circuitry [Damsohn et al., 2009]. After the development of the methodology, two-phase flow experiments have been conducted in various flow channels. But this conventional electrical methodology has limitation in applying dynamic temperature conditions since the conductivity of the liquid is affected by its temperature. Therefore, experiments with electrical methods have been limited to isothermal flow condition despite the fact that most two-phase flows in nuclear power plants involve heat transfer causing locally

varying temperature conditions. For an accurate analysis, experiments should include the temperature varying conditions such as phase change.

In this study, the limitation of the conventional electrical method is overcome by adopting a three-ring conductance method. The three-ring conductance method is proposed to measure the liquid film thickness in varying temperature condition with minimizing the error caused by temperature change. Electrode design of the three-ring conductance method is improved to make it suitable for patterning in dense area. To design and optimize the geometry of the sensor electrodes, the electrical potential field simulation is conducted with commercial code, COMSOL. The electrode design proposed in this paper has the ability to measure the liquid film thickness from 0.5 mm to 3.5 mm with a square spatial resolution of 15 mm × 15 mm. By fabricating the sensor on flexible printed circuit board (FPCB) the application of the sensor is extended to relatively high temperature and curved surface conditions.

In order to analyze the liquid film flow accurately, multiple measuring points are necessary. However, a large number of sensor demands a huge data acquisition system. In this study, a parallel circuitry system which is a modified and simplified form of the wire-mesh circuitry is devised to apply on three-ring method. This parallel circuitry allows the number of data acquisition channels to be reduced effectively.

A prototype sensor is manufactured in 6×6 array and calibration procedure for the prototype sensor is conducted. The calibration result is cross-checked with needle probe and ultrasonic thickness gauge to ensure the accuracy of the calibration. After confirming the feasibility of the liquid film sensor, a liquid film flow experiment is conducted with an extended liquid film sensor that can cover

wider film width and have more sensing electrodes than the prototype sensor. In this experiment, a signal switching device is adopted to measure the falling liquid film continuously. In addition, a modified current ratio form was proposed to extend the applicable temperature variation range.

……...

Keywords: Liquid Film Thickness, Liquid Film Sensor, Three-ring Conductance Method, FPCB (Flexible Printed Circuit Board), Two-phase Flow Experiment

Student Number: 2014-21423

List of Contents

List of Tables

List of Figures

Chapter 1.

Introduction

1.1 Background

Recently, the needs for high precision two-phase flow experiments are increasing in the nuclear safety field. Therefore, a lot of researches for two-phase flows in annular and pipe flow conditions have been conducted. As a liquid film flow developed in annular channel or pipe is one of major factors for the safety of nuclear power plants, various liquid film flow experiments were conducted.

As a measurement technique advances, researches regarding local liquid film thickness are brought up since the liquid film flow is frequently occurred in two-phase flow. For example, liquid film flow experiment was conducted to analyze annular flow in BWR fuel element [Damsohn et al., 2010]. Damsohn et al. (2010) measured local liquid film thickness covering the rod bundles to analyze the flow of the liquid film occurring in BWR fuel element. The flow condition of the experiment was limited to air-water flow and isothermal condition. This experiment was confined to an isothermal condition due to the limitation of the liquid film sensor, the local liquid film thickness was measured with high time and spatial resolution. Meanwhile, two-dimensional film flow experiment was conducted in the plane geometry condition [Yang et al., 2015]. The objective of this experiment was analyzing the behavior of the safety injection water during the reflood phase in

LBLOCA (Large Break Loss of Coolant Accident) situation. Also, the interfacial and wall friction factors were re-evaluated in this research. Fig. 1.1 represents the schematic diagram of experiment facility of two-dimensional film flow experiment [Yang et al., 2015]. The geometries of the test sections in this experiment are 1/5 and 1/10 scaled down of the unfolded downcomer. With blowing the air to lateral direction, local liquid film thickness and local liquid velocity were measured by using ultrasonic thickness gauge and PIV (Particle Image Velocimetry) technique. The experiment was conducted under two-dimensional plane flow channel and atmospheric air-water flow in isothermal condition. Thus, this experiment has confined the flow condition with considering the characteristics of downcomer flow condition. For extending the above experiment with more realistic conditions reflecting the real flow conditions, several flow conditions should be included.

At first, in the downcomer of the reflood phase, steam-water two-phase flow mainly occurrs rather than air-water flow. So, to examine the two-phase flow precisely, the working fluid should be replaced with steam and water.

Secondly, experiment should be carried out on the curved surfaces. The shape of the downcomer is not the plane geometry but the annular pipe shape. Different flow pattern is expected if the test section were replaced to the curved surface.

Thirdly, high precision data are necessary for more accurate analysis on the experiment. The local liquid film thickness was measured by using an ultrasonic thickness gauge in Yang's experiment. However, due to the probe size of the ultrasonic method, the distance between the measuring points was rather coarse (Width: 30 mm, Length: 30 mm).

Consequently, experiments should include the steam-water flow, curved test sections and higher resolution, besides the local data is demanded.

1.2 Literature Reviews

1.2.1 Measurement Methods for Measuring Liquid Film Thickness

There are various methods that can measure the liquid film thickness. Generally, ultrasonic, electrical, optical and neutron method are used to measure the liquid film thickness.

Ultrasonic method measures the liquid film thickness by time difference between the reflected signals from boundary interface of the medium. As the velocity of sound is affected by its medium, ultrasonic method has rather low precision. Furthermore, this method has limitation in measuring thin film thickness. Also, multiple point measurement with ultrasonic method is confined due to the high expense of the device [Alig et al, 2007].

Electrical method is widely used on two-phase experiments due to its applicability on measuring not only liquid film thickness but void fraction. Most electrical methods use the electric conductivity of the liquid to measure the liquid film thickness. In case of non-conductive liquids, capacitance method is applied to measure the film thickness. Generally, electrical methods for liquid film measurements have high time resolution due to the electrical characteristics. However, relatively low spatial resolution was a limitation of the electrical methods because of the electrode geometry.

There are high speed camera, diffraction and X-ray tomography among the optical methods. Though most optical methods have a high spatial and time resolution, there are limits on applying it to complicated flow condition as the light is distracted in boundary interface [Takahama et al., 1980].

Neutron based method usually measures the film thickness by tomography

technique. Though the spatial resolution of this method is considerably high, it can only provide time-averaged data. Also, it demands lots of expense to set up the measurement device.

1.2.2 Electrical Method for High Time and Spatial Resolution

Damsohn et al. (2010) applied the electrical method on the PCB (Printed Circuit Board) in order to measure the local liquid film thickness as shown in Fig. 1.3. Since the PCB allows the elaborate fabricating of the electrode, the limitation of electrical method regarding the spatial resolution was resolved. The maximum measurement thickness of the sensor was 1.0 mm with a square spatial resolution of 2.0 mm × 2.0 mm. By coupling the sensor with the wire-mesh circuitry system (Prasset et al., 1998), high resolution on time and space was achieved. Explanation about wire-mesh circuitry will be covered in Chapter 3.3. After this method was developed, the electrode of the electrical method also was fabricated on the FPCB (Flexible Printed Circuit Board) to be applied on annular flow as shown in Fig. 1.4. Also, research for measuring very thin liquid film was conducted with FPCB and electrical method [D'Aleo et al., 2013].

Though coupling the FPCB or PCB with wire-mesh circuitry provides high resolution of time and space at the same time, the experiment condition was confined to isothermal condition. As the electric conductivity of the liquid is affected by its temperature, electrical method cannot be applied on the experiments in which the local temperature of the liquid changes. Generally, electric conductivity of the water increases about 2% when the water temperature increases 1^{o}C [Hayashi, 2004]. Thus, the conventional electrical method cannot be applied on the two-phase flow experiment which involves the heat transfer.

1.2.3 Three-ring Conductance Method

The three-ring conductance method was proposed by Coney (1973). As this method is based on the conventional electrical method, it has similar characteristics of the electrical method. As illustrated in Fig. 1.5, three-ring method has three electrodes (transmitter and receiver-1, 2). By using the current ratio (I_1/I_2), liquid film thickness can be measured under temperature varying condition since the current ratio compensates the change of electric conductivity. Kim et al. (2013) conducted experimental research about three-ring conductance method for the liquid film measurement in varying temperature condition. However, as the three-ring conductance method by Kim et al. (2013) was fabricated on the PCB, it has limitations in applying high temperature condition or curved surface condition.

1.2.4 FPCB

FPCB which Damsohn et al. (2010) and Arai et al. (2014) applied on liquid film sensor is widely used on IT (Information Technology) and MEMS (Micro Electrical Mechanical System) field. To extend the application area, plastic insulated substrate of PCB is replaced with PI (Polyimide) film. The PI film has high flexibility and tolerance on relatively high temperature (150^{o}C) condition [Peter, 2002]. Also, as the FPCB is based on PCB technology, multi-layer fabrication and elaborate electrode design is possible. Due to these characteristics, various measurement techniques have been developed in mechanical engineering field. Pritchard et al. (2008) applied the capacitance pressure sensor on FPCB so as to develop the pressure sensor with high spatial resolution. Shikida et al. (2012) coupled the FPCB

with MEMS system to develop the sensor which can measure the velocity of the air. Dainel et al. (2007) devised the sensor which can measure the local temperature and strain together.

1.3 Objective of Study and Scope

Until now, there is no measurement method for liquid film thickness that satisfies the application on high temperature, varying temperature condition, curved surface and high resolution on time and space. Therefore, in order to conduct the experiment considering downcomer flow conditions, a new liquid film sensor that satisfies above conditions should be developed.

The objective of this study is developing a new liquid film sensor which overcomes the limitations of previous methods. For the measurement under varying temperature condition, three-ring conductance method was adopted to overcome the limitation of the general electrical method. To achieve the high spatial resolution, FPCB is applied for fabricating the electrodes of the three-ring conductance method. The newly designed liquid film sensor was validated by calibration process. Also, to verify the application of the developed sensor, a liquid film experiment was conducted by using the liquid film sensor.

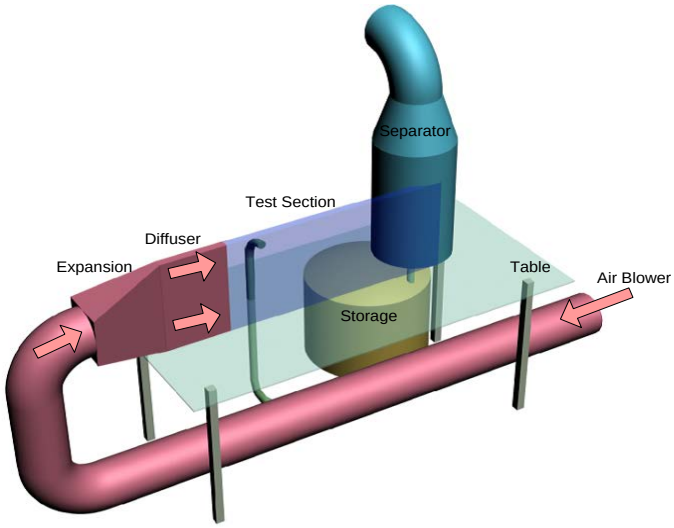

Figure 1.1 Two-dimensional film flow experiment (Yang, J. H. et al., 2015)

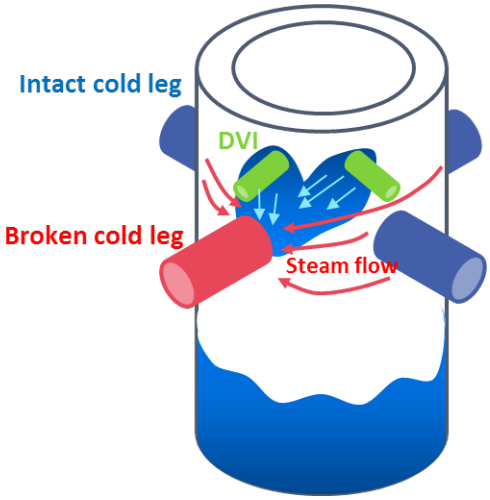

Figure 1.2 Behavior of safety injection coolant during Reflood phase in LBLOCA

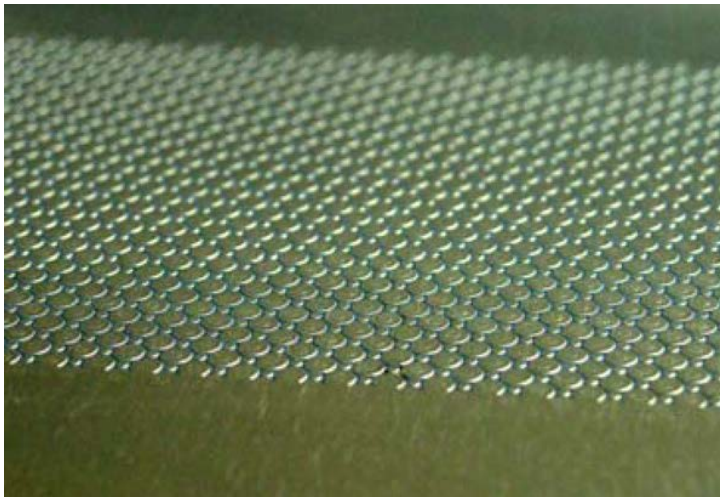

Figure 1.3 Liquid film sensor based on PCB (Damsohn et al., 2010)

Figure 1.4 Liquid film sensor based on FPCB (Arai et al., 2014)

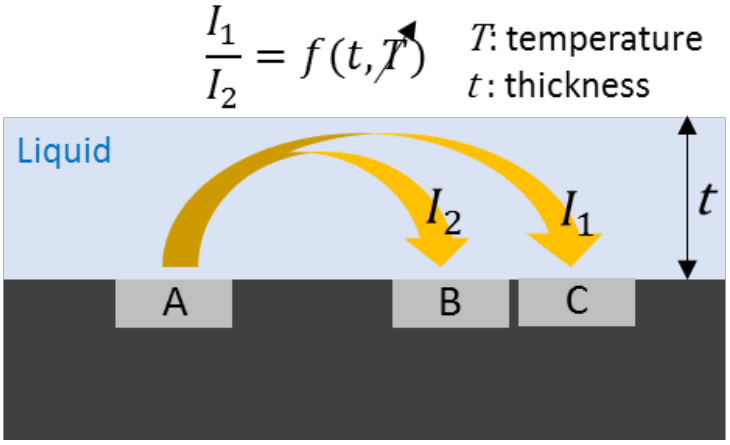

Figure 1.5 Principle of three-ring conductance method (Kim et al., 2013)

Chapter 2.
Preliminary Experiment for Three-ring Method on FPCB

2.1 Theory of Three-ring Method

The conventional electrical method measures the liquid film thickness by using the current flowing from transmitter electrode to receiver electrode (Fig. 2.1). In case of liquid film thickness measurement, the electrical resistance is dependent on the film thickness if the temperature of the liquid is fixed. Therefore electrical method can measure the film thickness only under isothermal condition.

The three-ring method uses the current ratio to measure the film thickness as presented in Fig. 1.4. Since the current ratio compensates the temperature change, the measurement error could be minimized under temperature varying condition. The theoretical background of three-ring method is as follows. Assuming that an impedance of the liquid film has resistance property without reactance (inductance or capacitance), the impedance of liquid film is a function of temperature and thickness. Since the electric conductivity is a function temperature, an impedance ratio of A-B and A-C is only related to the film thickness, if the temperature of A-B and A-C is same. Previously there was a research to realize the three-ring method to liquid film sensor, where conceptual experiment was conducted with the

electrodes fabricated on the PCB [Kim et al., 2013]. Fig. 2.2 shows the design of electrodes proposed by Kim et al. (2013). To examine the function of the three-ring method, the current ratio was measured with the varying liquid film thickness and temperature. From this experiment, it was identified that the current ratio is proportional to film thickness and the electrode geometry has an effect on the result. Besides the function of temperature compensation was confirmed in the experiment.

2.2 Feasibility Test for Three-ring Method with FPCB

To examine the feasibility of the combining the three-ring method with FPCB, preliminary experiment was conducted. Based on the conventional design proposed by Kim et al. (2013), the electrodes were fabricated on FPCB. The specific dimensions of the electrodes are described in Fig. 2.2. The transmitter electrode is located on the left side in rectangular shape, and the receiver-1, 2 electrodes is placed on the right side with 0.1 mm gap being located between two receiver electrodes. Ground electrode is disposed on the top and bottom of the receivers to prevent an end effect with leaving 0.1 mm gap between receivers and ground electrode. The end effect means a bypass current generated around the edge of electrode. In order to confirm the geometry effect, two different size of electrodes (a=1.0 mm, λ =3 and a=1.0 mm, λ = 5) were manufactured.

The current ratio was measured by the circuitry system as represented in Fig. 2.3. AC 0.1V is induced to the transmitter in 1 kHz frequency. The reason for using AC signal is to prevent the polarization which deteriorates the electrode conductivity. If DC is induced to electrodes, impurities are concentrated on the surface of the electrodes. Then the conductivity of the electrodes changes, and it is

impossible to obtain constant current signals. In case of AC, as the positive and negative poles alters continuously, the polarization effect could be excluded. The frequency applied on this experiment is determined based on the previous research (Kim et al., 2013), this frequency reduces frequency effect (inductance and capacitance) of AC usage. In order to measure the current values accurately, Lock-in Amp is applied in this experiment as the Lock-in Amp supplies the filtered signals from external noise. AC signal induced to transmitter and current signals produced by receivers are transferred to Lock-in Amp. And the DAS (Data Acquisition System) acquires the output signals from Lock-in Amp.

As shown in Fig. 2.4, in the constant liquid film thickness by insulated acrylic block, current ratio is measured. Fig. 2.5 presents that the current ratio increases with the increasing the liquid film thickness. The inclination of current ratio gradually decreases with increasing film thickness. Also, it was found that the characteristic curves of current ratio are affected by electrode geometry. This geometry effect result represents that the customized design is required considering its measurement range. During the temperature of water changed from 30^{o}C to 60^{o}C, the output signals of I_1 and I_2 increased 47% and 45% respectively. This result shows that the single receiver method is not proper in varying temperature condition. In contrast with the individual currents, the current ratio was maintained at an almost constant value. It was confirmed that, the current ratio is independent of temperature change.

From the preliminary experiment, the availability of three-ring method on FPCB was proved. Also, the temperature independency of three-ring method was confirmed. Besides the necessity of customized electrode design depending on film thickness was found.

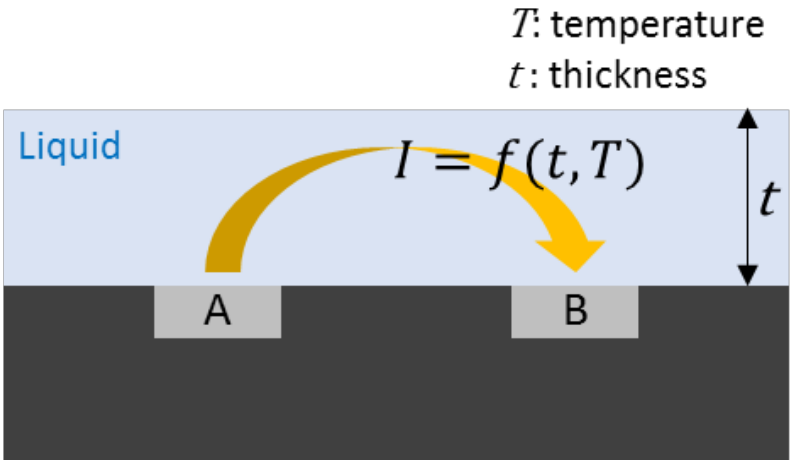

Figure 2.1 Conventional electrical method for measuring liquid film thickness

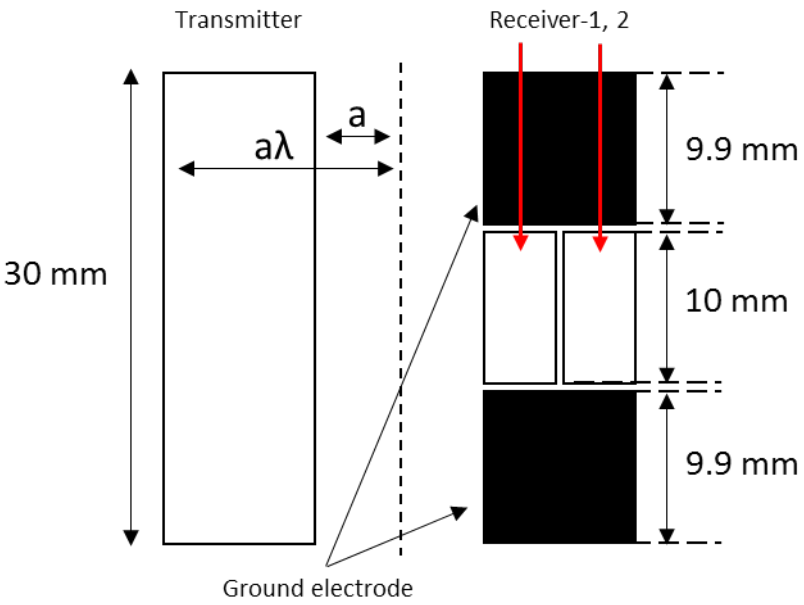

Figure 2.2 Electrode geometry of previous three-ring method

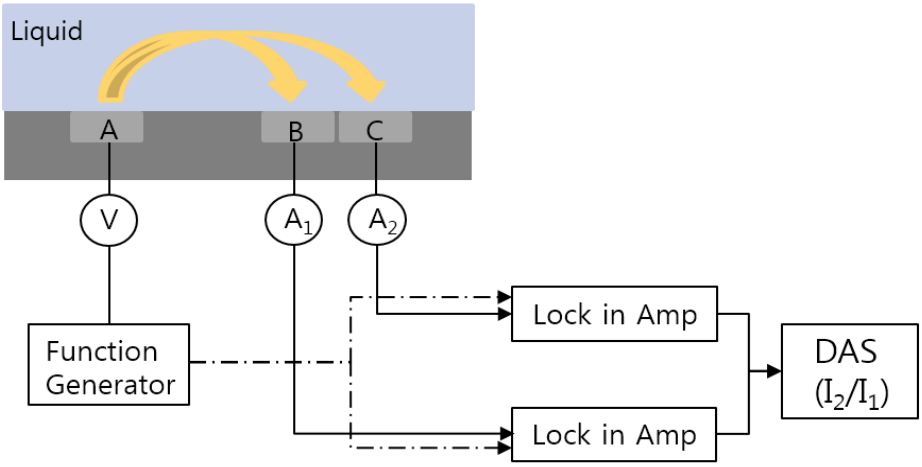

Figure 2.3 Circuitry system of preliminary test

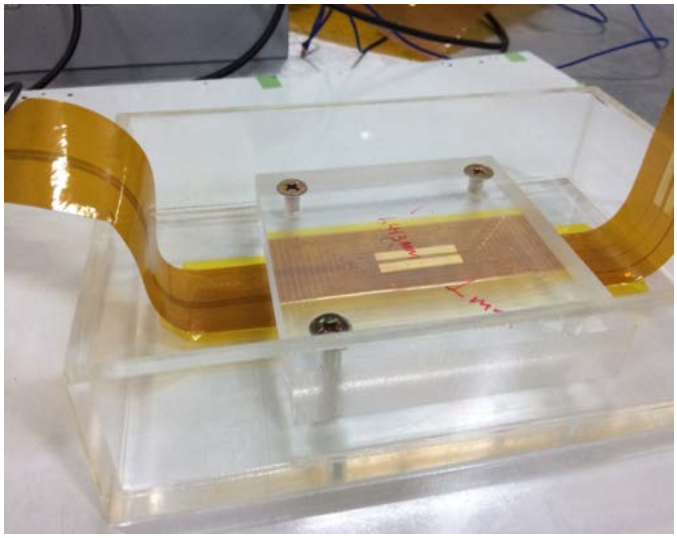

Figure 2.4 Constant liquid film thickness with acrylic block

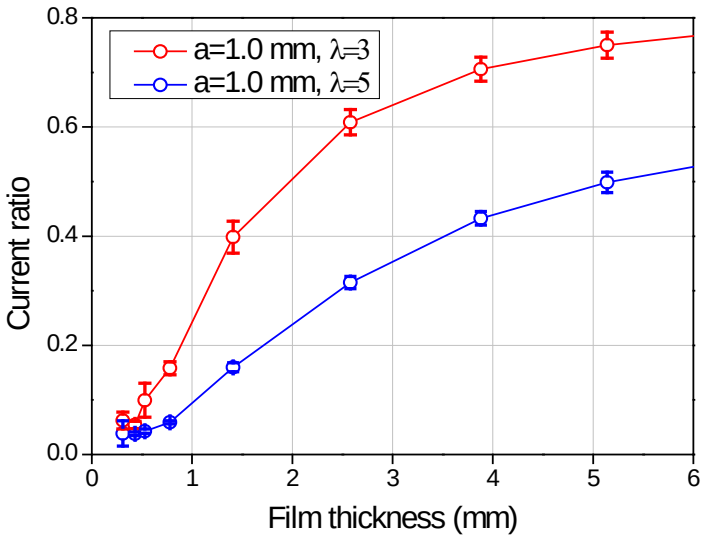

Figure 2.5 The current ratio with changing film thickness and electrode geometry

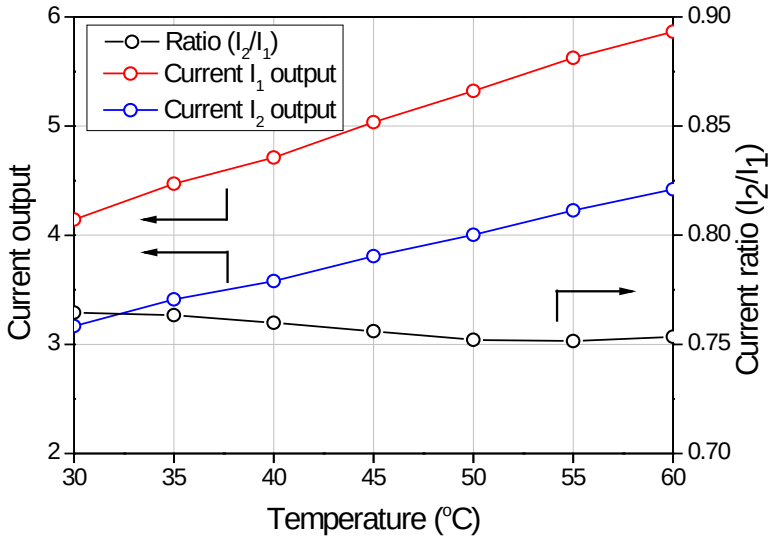

Figure 2.6 The current output signal and current ratio with varying temperature

Chapter 3.

Design Process of Liquid Film Sensor and Calibration

3.1 Electrical Potential Analysis for Electrode Design

The previous electrode design of three-ring method has difficulty in high spatial resolution because the electrode size is relatively coarse (30 mm length). Besides, electrode arrangement is not appropriate in composing an integrated system.

In this study, modification of the electrode design was carried out in order to achieve high spatial resolution. Fig. 3.1 shows the three-ring method of ring-type proposed in this study. The transmitter electrode locates in the center of a concentric circle and the receiver-1, 2 are placed with enclosing the transmitter. Because of the enclosed geometry, the ring-type arrangement can prevent the end effect without the ground electrode. Besides, the electric current flow pattern is radial symmetry so that it is easy to arrange the multiple sensors as presented in Fig. 3.2.

In order to design and optimize the geometry of the sensor electrodes, the electrical potential field simulation was conducted by using COMSOL Multiphysics ver. 5. 1 (COMSOL, 2015).

The electrical potential field developed in liquid film can be analyzed with solving the Maxwell equation:

$$\oiint_{\partial\Omega} E \cdot dS = \frac{1}{\epsilon_0} \iiint_{\Omega} \rho dV \quad (3\text{-}1)$$

$$\nabla \cdot E = \frac{\rho}{\epsilon_0} \quad (3\text{-}2)$$

Eqs. (3-1) and (3-2) are integral and differential formulation respectively, which represent the gauss law of the electrical potential. The meaning of the Eq. (3-1) is that the electric flux out of enclosed surface is proportional to the total charge of the enclosed surface, where E is electric field and $\boldsymbol{\varepsilon_o}$ is the permittivity of free space. Eq. (3-2) means that the net enclosed charge can be measured with the electric field. Eqs. (3-1) and (3-2) are mathematically equivalent by the divergence theorem.

In order to confirm the relation of electrode geometry and the current ratio, electrical potential field simulation was conducted with changing the radius of the electrode. The target measurement thickness is 0.5 ~ 3.0 mm which is the range of Yang et al. (2015)'s Experiment.

Fig. 3.3 shows the calculation domain of COMSOL simulation. Plane water film with electric conductivity covered the ring-type electrodes, and the other boundary of the bottom plane was set to insulated plane. 1V electric potential was applied on the transmitter electrodes, and the receivers were set to ground potential.

Electrical potential field was developed as presented in Fig. 3.4. The electric flux diffused from the center transmitter and converged to the two receivers. Especially, the electric flux was concentrated on the near region which means the shallow film thickness. The current ratio becomes larger and the slope is saturated to zero as the film thickness increase (Fig. 3.5). In order to confirm the current ratio consistency regardless of the conductivity, calculations with different water conductivity were conducted. And it was found that the current ratio is not related with electric conductivity.

Fig. 3.5 shows the current ratio curves with increasing the outer radius of ring type sensor. Generally, large probe can measure thicker film since the saturation point is delayed to the thicker region. This result indicated that enlarging the probe size is desired for measuring the thick liquid film. And the similar conclusions were found in the previous studies with the conventional electrical method [Damsohn et al., 2009].

Since the target thickness range of this study is 0.5 ~ 3.0 mm which is based on experimental result of Yang et al. (2015), the outer radius size was determined to 4.5 mm. A series of calculations were conducted to confirm the specific dimensions of the electrodes. Finally, the specific dimensions of the ring-type electrode were confirmed as presented in Fig. 3.6.

Generally, in case of composing the multiple sensors in small area, unintended currents are developed on the far receivers which is belonged to neighboring probes [Vasilescu et al, 1999]. This unintended leakage current is called the cross-talk. As the cross-talk distort the signal of the sensor, ground electrode is required to absorb the leakage currents.

In this study, the probes were uniformly distributed with 15 mm pitch, and the ground electrode is inserted between the probes as shown in Fig. 3.7. The shape of ground electrode was selected to a lattice with narrow width. To determine the width of the ground electrode, additional electric potential calculation was performed with the geometry as illustrated in Fig. 3.8. With increasing the width from 0.2 to 4.0 mm, the current ratio of the 1^{st} probe and the cross-talk current developed in 2^{nd} probe were calculated. Although the cross-talk current decreased with increasing the width, the saturation thickness of the current ratio became thinner. In result, the width of ground electrode was determined to 0.2 mm and the characteristic curve

of the ring-type sensor is expected with Fig. 3.10.

3.2 Parallel Circuitry for Three-ring Method

In order to acquire the data from the three-ring method, three signal lines for each probe (one for transmitter and the others for receiver-1, 2) are required with general signal processing methods. In case of multiple sensor system such as N×N array, $3N^2$ signal lines are required and this amount of signal lines also demand an uneconomically massive DAQ (Data Acquisition).

Wire-mesh circuitry system has the circuit pattern presented in Fig. 3.11 that can address the above problem with crossing the signal lines of transmitters and receivers [Damsohn et al., 2010]. The transmitter electrodes located in the same row are connected in parallel, and the receiver electrodes located in the same column are coupled in parallel. The inducing signal is supplied to the first transmitter line and measuring is conducted in the sensors which are connected to the first transmitter line. After measuring and recording are finished, the inducing signal is switched to next transmitter line. As a result, the data of whole sensors can be produced by successive switching the transmitter lines and therefore, the number of signal lines can be reduced to 2N for the N×N array sensor system. In addition, real time measurement is also possible, if the switching frequency is high enough to detect the flow pattern.

However, the above wire-mesh circuitry was designed for the sensors composed with two electrodes. Thus, it is required that modifying the circuitry pattern to apply on three-ring method. In this study, the circuitry system is modified as illustrated in Fig.3.12. For the N×N array sensor system, N signal lines are deposed for

transmitters and 2N signal lines are deposed for receivers. The signal lines of transmitter and receivers are crossed with similar pattern of the wire-mesh circuitry. Voltage signal (AC sine wave) is induced to transmitter line and 2N of receiver lines transfer the currents, and the measurement for liquid film thickness is proceeded successively with changing the connecting nodes.

3.3 Prototype Sensor and Calibration

Based on the electrode design which was determined by electrical potential calculations, the prototype sensor was fabricated on FPCB with 6×6 array of probes as shown in Fig. 3.13. The dimension of the prototype sensor is 95 mm × 300 mm width and length, the dimension of the measurement part is 90 mm × 90 mm width and length. The circuitry layout of the prototype sensor is presented in Fig. 3.14. Total thickness of the FPCB sensor is about 330 μm and there are little grooves (30 μm) between the electrodes and PI film. Material of the electrode is copper and the top surface of the electrode is coated with gold and nickel to prevent the corrosion from water. In addition, as the FPCB is composed with 4 layers, each kind of signal lines was separated regardless of short circuit (Fig. 3.15).

3.3.1 Calibration with Isothermal Condition

To examine the performance of the prototype sensor, calibration was performed with using the calibration device which is shown in Fig. 3.16. To maintain the constant distance between FPCB sensor and insulated plane, transfer device was installed. Through the gap between the insulated plane and the FPCB sensor, liquid

film with uniform thickness was developed, and the currents flowing to the receivers were measured. The specific process of the calibration is described in Fig. 3.17.

The water used in the calibration device was circulated continuously by the pump to keep the uniform composition. In addition, electric conductivity and temperature of the water was measured. The transfer device is connected with micro-screw which has 0.01 mm spatial resolution so that the film thickness can be controlled accurately. The signal processing system of this calibration is shown in Fig. 3.18. Transmitter line is connected to the function generator and the receiver lines are connected to ground potential through the resistors. DAS reads the voltage signal from both ends of the resistor instead of the currents signal.

The physical and electrical condition of the calibration is as follows. 10V, AC sine wave signal with 1 kHz frequency is induced to transmitter line. Temperature and electric conductivity of the water was 22^{o}C and 5 μS/cm respectively. The calibration range was 0.0 ~ 4.0 mm with 0.5 mm step.

In general, measurement of the electrical signal is easily distorted by external electric noise. Especially in case of measuring fine signals, precise measurement is hard as the scale of noise level is too large to detect the original signal. To avoid the signal interruption from external noise, a band-pass filter function built in LabVIEW 2009 (National Instruments) was applied on this study. The role of band-pass filter function is cutting off the signals which are out of designed frequency range. And by using this function, external noise with high and low frequency was blocked effectively so that the signal of inducing frequency can be measured accurately.

36 sensors of prototype was assorted by the signal lines as shown in Fig 3.19.

Transmitter lines are classified with line 1 ~ 6, receiver lines were classified with A ~ F and a ~ f. In addition, the location of the sensor was classified by using 1~6 and A~F lines.

3.3.2 Calibration Result of Isothermal Condition

The calibration was performed to obtain 36 different calibration curves as the 36 sensors do not have identical characteristic. This feature was also found in analysis on PCB liquid film sensor [Damsohn et al, 2009] and this result is considered as fabrication tolerance of the FPCB.

The calibration results of the sensors locating 2-A and 3-D are presented in Fig 3.20 and 3.21. Trend of the current ratio curve is analogous with the COMSOL simulation result. The current ratio becomes larger while increasing the film thickness and saturates at the region above 3.5mm. In other words, the sensor can measure the film thickness up to 3.5 mm. As a result, the target measuring range (0.5 ~ 3.0 mm) was achieved. The major difference with simulation result is an offset point at zero film thickness which is caused by water filling the grooves (about 30 μm) between electrodes and PI films. This result was also found by Damsohn et al. (2010) and it does not have major influence on measuring film thickness.

For measuring the liquid film thickness by using the calibration result, thickness curve which is the function of current ratio is required. By adapting the polynomial fitting method, 4^{th} order of polynomial function is expressed as:

$$T = \mathrm{a}R^4 + \mathrm{b}R^3 + cR^2 + dR + e \qquad (3\text{-}3)$$

Where, R and $a \sim e$ are expressed as:

$$R = \frac{I_1}{I_2} \tag{3-4}$$

$$a, b, c, d, e: \text{constants from polynomial fitting} \tag{3-5}$$

To clarify the repeatability of the sensor, five independent tests were conducted under equivalent test conditions. As presented in Fig. 3.20 and 3.21, the calibration results show that the error of the current ratio is less than 3%. And main reason of this error is considered as an electrical noise.

In order to validate the calibration result, additional tests with comparing other measurement methods were conducted.

Needle probe test

Fig. 3.22 shows the process of needle probe test. Camera captures the moment that the needle touches the surface of the liquid film. With controlling the liquid film thickness, a series of measurements by the liquid film sensor and needle were conducted coincidentally. The results are plotted in Fig. 3.23. The X-axis represents film thickness that measured by needle probe mechanically and Y-axis represents thickness measured by liquid film sensor. Although the results show that relatively high discrepancy occurs in certain points, the average error was 3.5% and discrepancy is not biased.

Ultrasonic thickness gauge test

The validation was also conducted with ultrasonic thickness gauge. The principle of the ultrasonic thickness gauge is described in Fig. 3.24. Ultrasonic wave

generated from the probe is reflected at the interfacial boundary of the medium that waves passes. The probe detects the reflected waves and measures the thickness of the medium by the time difference between waves from medium boundaries of both ends. Fig. 3.25 shows the comparison results between liquid film sensor and ultrasonic thickness gauge. The maximum error between two methods was 5.3% and the average error was 1.8%. Besides the result around 4.0 mm shows good agreement. By using this result, the measurement range of 0.5 ~ 3.5 mm is confirmed.

From these comparisons with other methods, the calibration result and process were validated.

Measurement requirement

Current ratio is expected that it is independent of conductivity. In fact, the theory of three-ring method has an assumption that the water has only electric conductivity without any other impedance properties such as reactance or capacitance [Kim et al., 2013]. In other words, the compensation effect of the electric conductivity by current ratio is confined to identical water composition and narrow range of temperature because the reactance and capacitance properties are also varied by temperature change. This is also clarified on previous study about the three-ring method [Kim et al., 2013] Therefore, to measure the liquid film thickness based on calibration result, experiment should be conducted with the identical water used in calibration.

3.3.3 Calibration with Temperature Variation

For estimating the applicability of the liquid film sensor on temperature varying condition, the current and current ratio are measured with increasing the water temperature (22 ~ 60^{o}C). Increasing the water temperature makes the conductivity rise and the resistance of liquid film decrease. Consequently, the currents flowing to the receivers increase as shown in Fig. 3.26 and 3.27. Theoretically, current ratio should be maintained regardless of temperature change, but the result from experiments is separated as shown in Fig. 3.28. The range of temperature compensation is confined to 10^{o}C change with a certain error.

The reason of separated current ratio is that the currents flowing to the receivers are not consistent with temperature change. In order to clarify the reason, impedance of the liquid film was measured by LCR meter. Fig. 3.29 shows the impedance change rate (60^{o}C compared to 22^{o}C). The decrease rate of impedance is irregular around the 0.5 mm region compared to 2.0 ~ 3.5 mm region. And this irregular pattern of the impedance change makes the current ratio not to be converged. Since the three-ring method uses AC signals, measuring the resistance and impedance of the film was also conducted to find out the effect of frequency. As presented in Fig. 3.30, over the 99% of the impedance is composed of resistance property. This result implies that the effect of frequency is little in this irregular impedance change. As a result, using the liquid film sensor directly on temperature varying condition is limited.

However, it is necessary to extend the temperature varying range for the application on experiments including heat transfer. In this study, a modified current ratio was proposed to improve the temperature compensation function of three-ring

method. It is required that the variable of the modified form should be limited to I_1 and I_2 since the measurement values produced by the sensor are I_1 and I_2. As shown in Fig. 3.29, the current ratio changes the most when the film thickness is around 1.0 mm. At this point, the increasing rate of I_2 is larger than that of I_1 when temperature increases. To maintain the current ratio consistent, a part of I_2 is added to the denominator I_1. In here, as the current ratio value increases, the discrepancy becomes smaller. A new modified current ratio form was proposed as follows:

$$R^* = \frac{{I_2}^{\alpha}}{(C_1 \cdot I_2 + I_1)^{\beta}} \tag{3-6}$$

Where, C_1 and α, β are expressed as:

$$C_1 = 0.9 \cdot (1 - tanh(10R - 8)) \tag{3-7}$$

$$\alpha = 0.8 + 0.07 \cdot (1 - \tanh(6R - 5)) \tag{3-8}$$

$$\beta = 1.1 - 0.000787e^{R/0.1728} \tag{3-9}$$

The coefficients of Eqs. (3-7) ~ (3-9) are determined empirically based on calibration data.

A modified current ratio shows better converged data compared with the previous current ratio form as plotted in Fig. 3.31. Besides, the difference between maximum and minimum value of ratio was maintained compared to that of previous current ratio form. Based on the averaged current ratio, calibration curve was determined and the measurement error is presented in Fig. 3.32. On average the measurement data has 7% error range and the temperature varying range enlarged to 20^{o}C change.

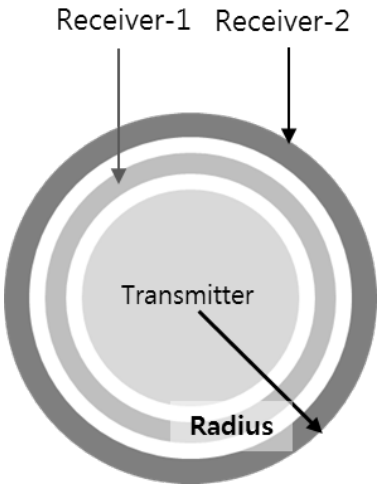

Figure 3.1 Ring type electrode of three-ring method

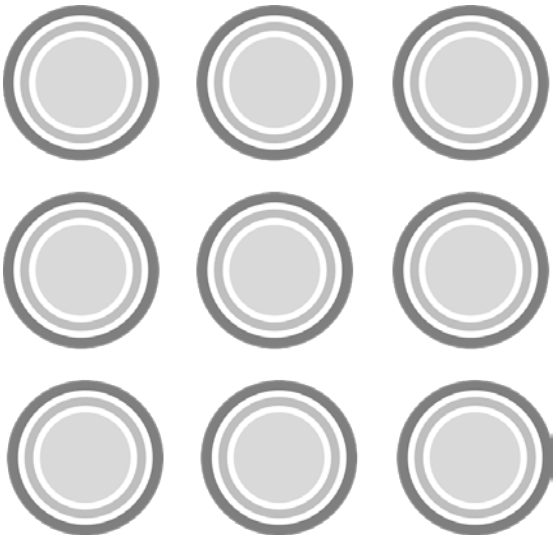

Figure 3.2 Pattern of multiple three-ring sensor

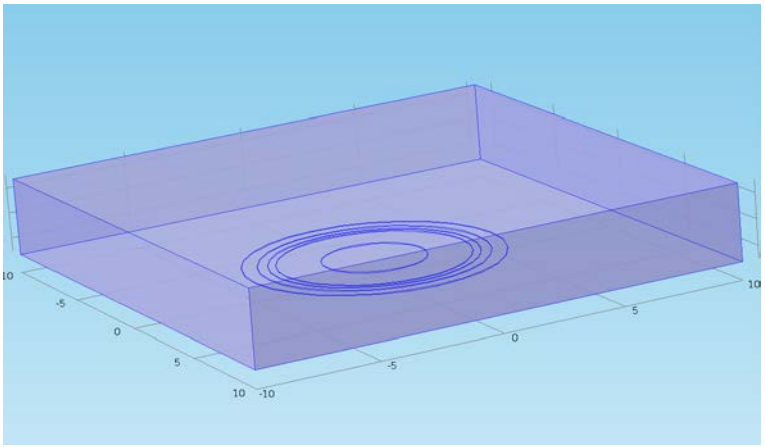

Figure 3.3 Geometry of electrical potential analysis using COMSOL

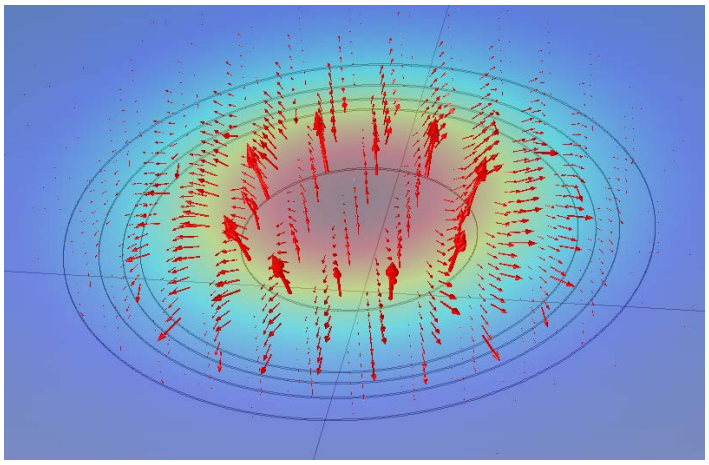

Figure 3.4 Electrical potential distribution of ring type three-ring method

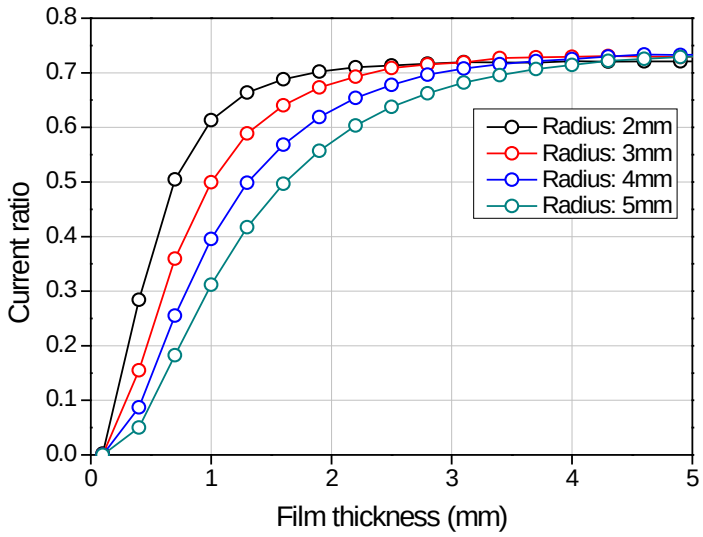

Figure 3.5 Electrical potential field calculation result according to radius sized

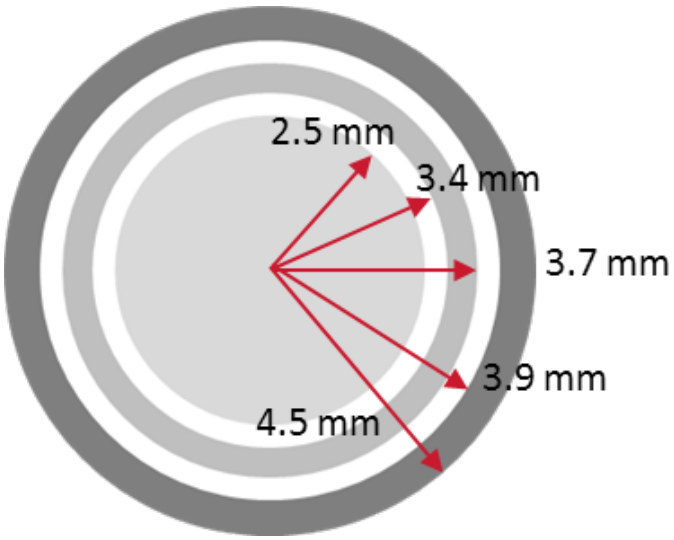

Figure 3.6 Specific dimensions of ring type sensor

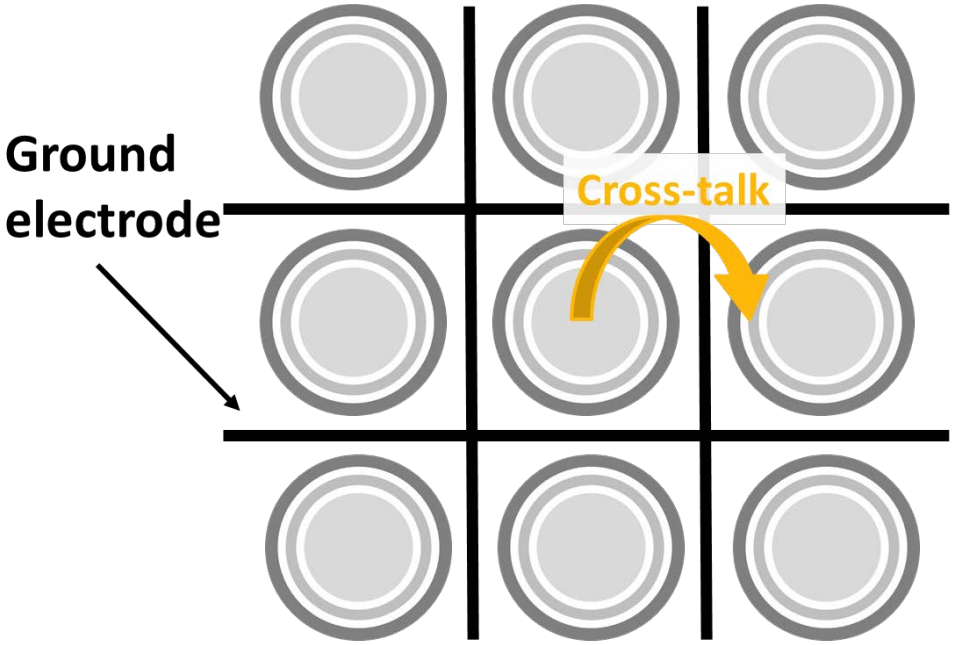

Figure 3.7 Arrangement of ground electrode to prevent the cross-talk current

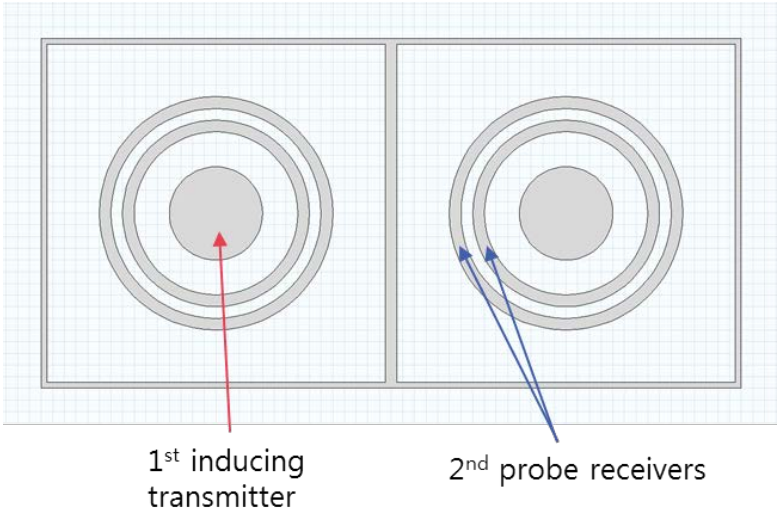

Figure 3.8 Probe array for calculating the cross-talk current

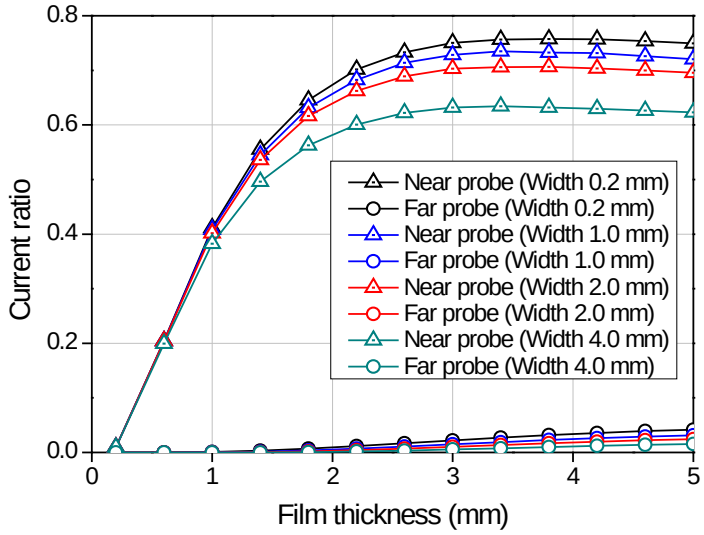

Figure 3.9 Electrical potential field calculation result regarding with the width of ground electrode

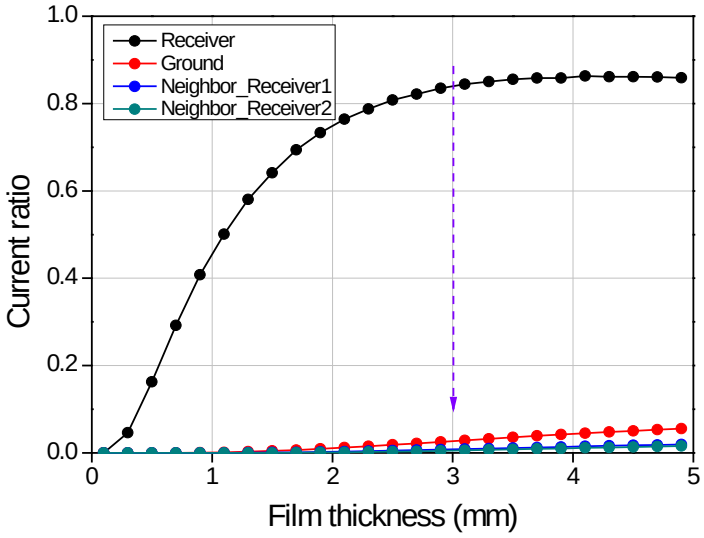

Figure 3.10 Characteristic curve of the confirmed design

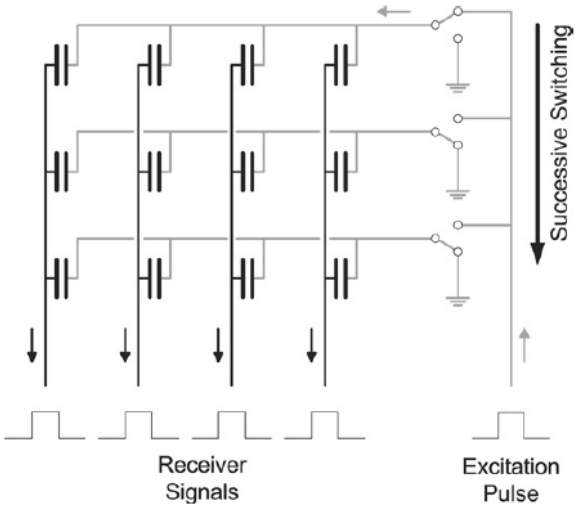

Figure 3.11 Circuitry of the coupling wire-mesh with electrical method (Damsohn et al., 2010)

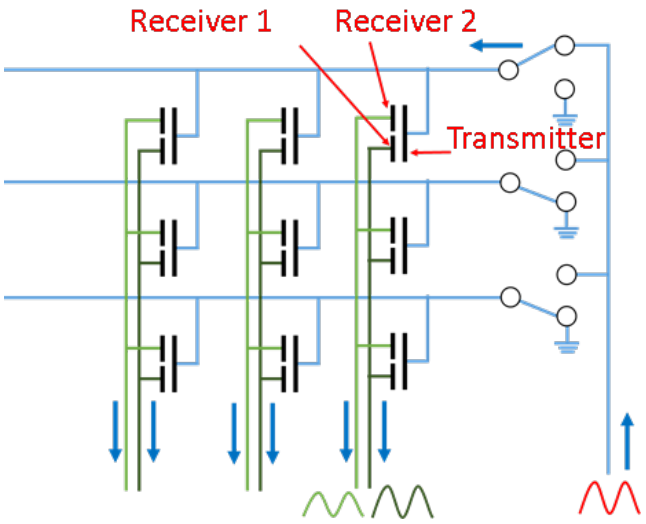

Figure 3.12 Parallel circuitry system for three-ring method

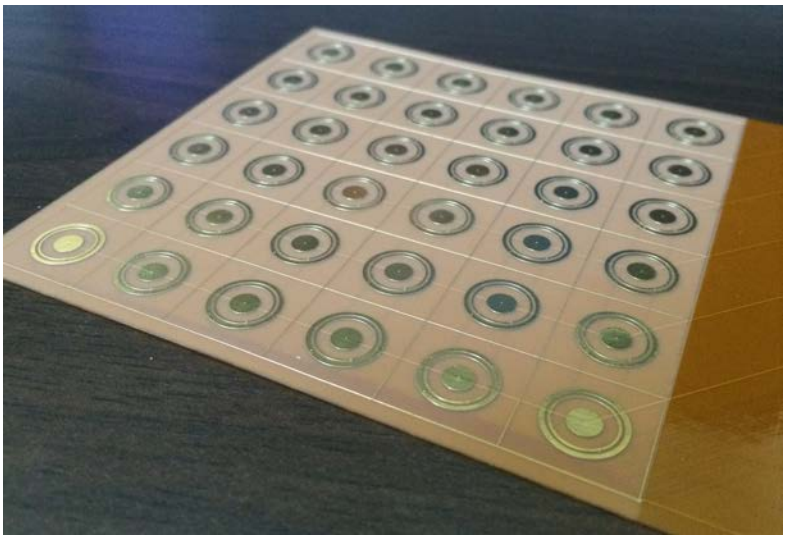

Figure 3.13 Prototype sensor (6×6 array)

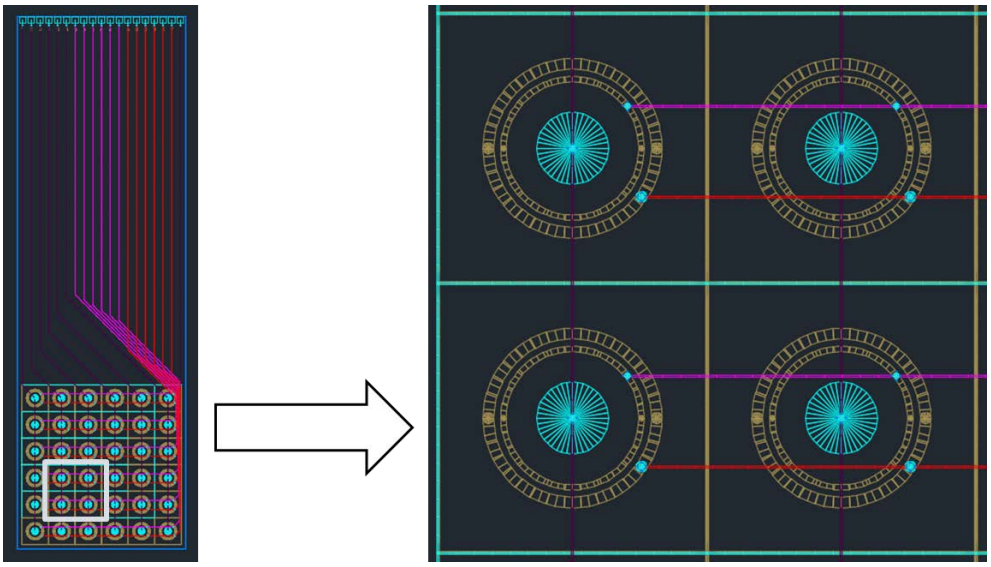

Figure 3.14 Layout of the detailed circuit composition

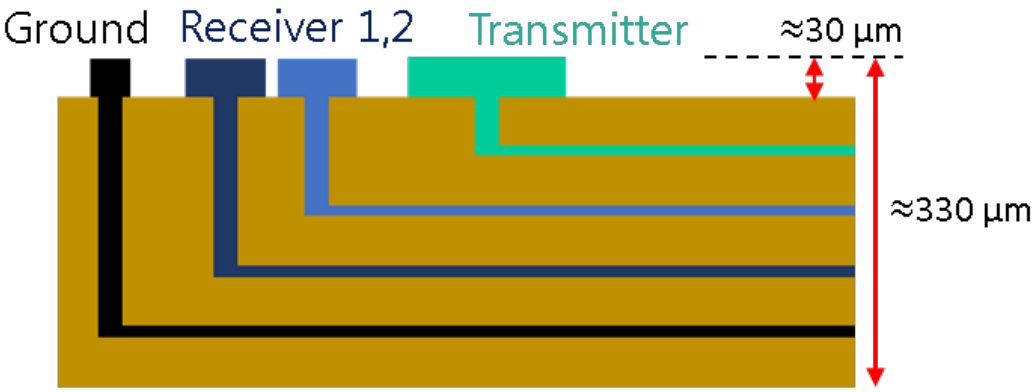

Figure 3.15 Cross-sectional view of the prototype sensor

Figure 3.16 Calibration device for prototype sensor

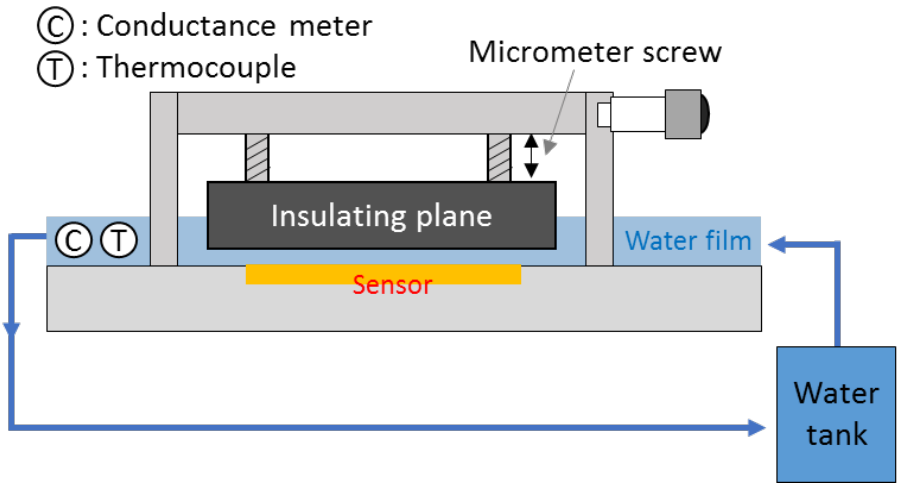

(a) Side view of the calibration device

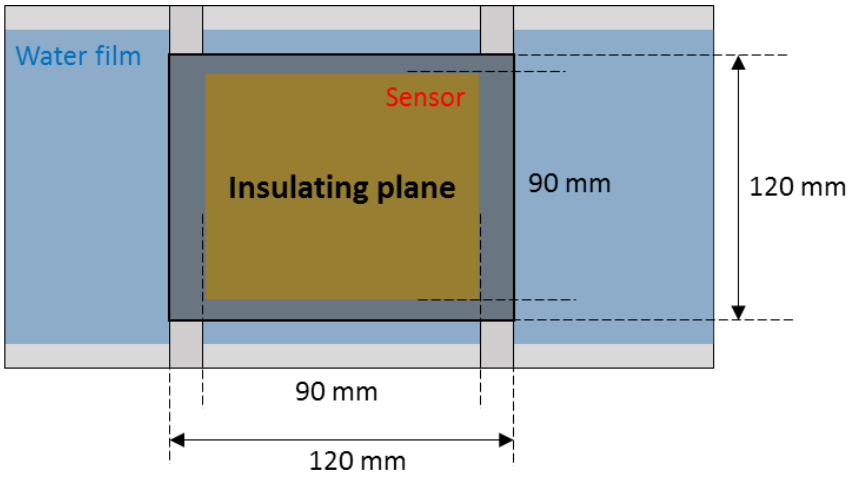

(b) Top view of the calibration device

Figure 3.17 Specific dimensions of calibration device

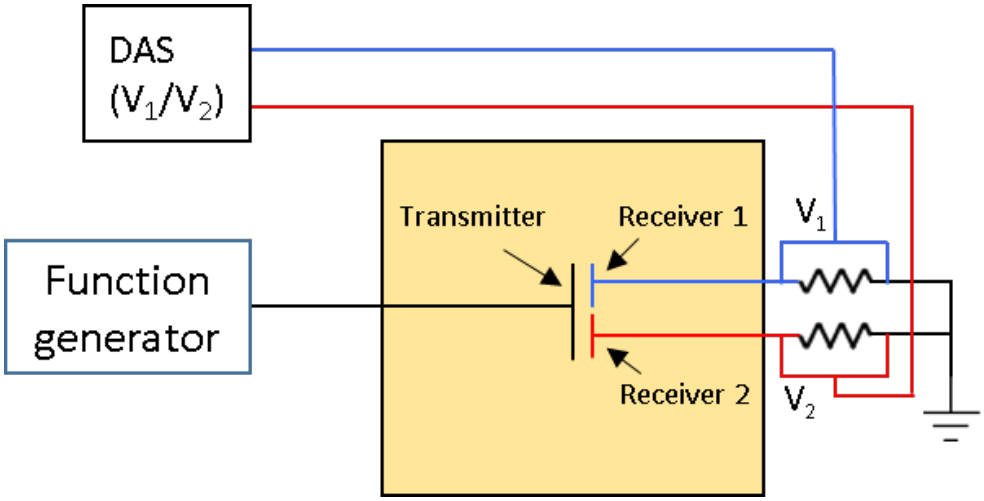

Figure 3.18 Circuitry system for measuring the current of prototype sensor

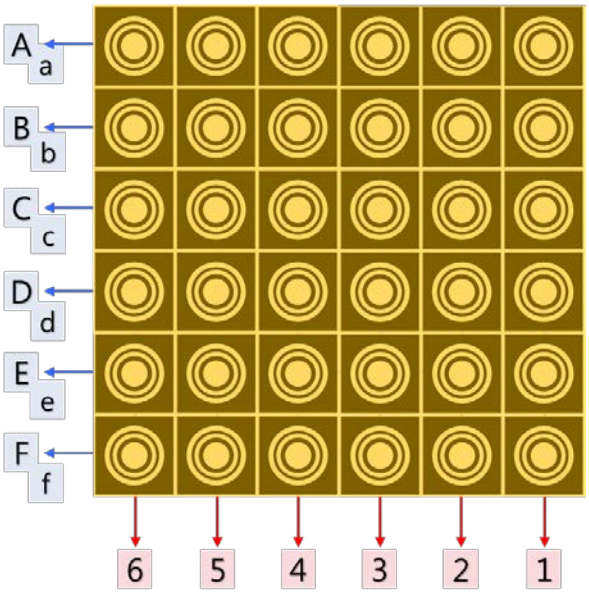

Figure 3.19 Classification of transmitter and receiver circuit

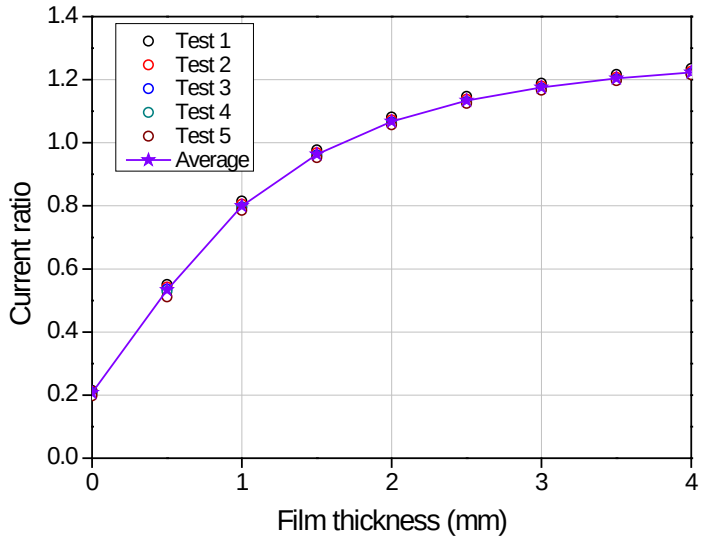

Figure 3.20 Calibration result (Probe 2-A)

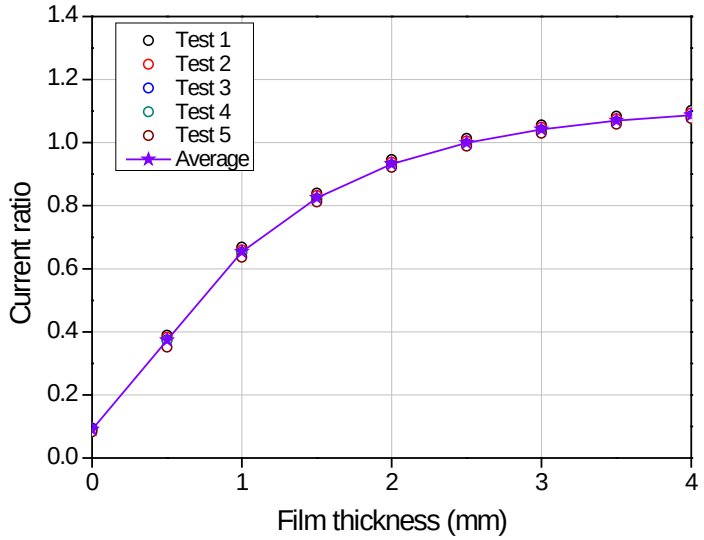

Figure 3.21 Calibration result (Probe 3-D)

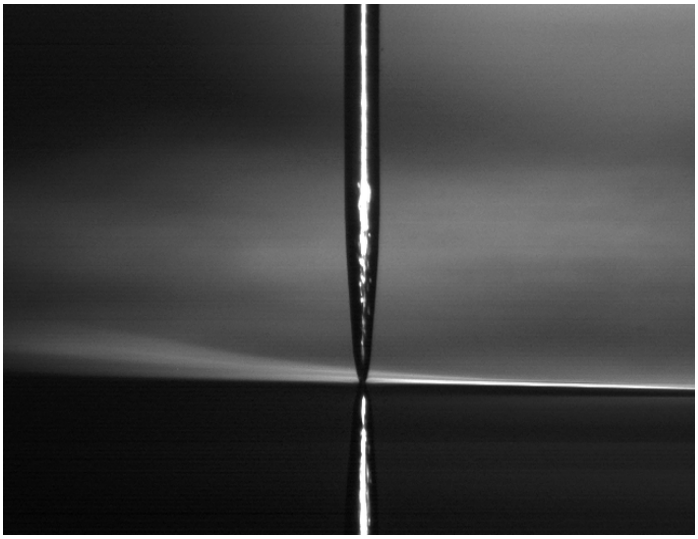

Figure 3.22 Measurement of liquid film thickness using needle probe

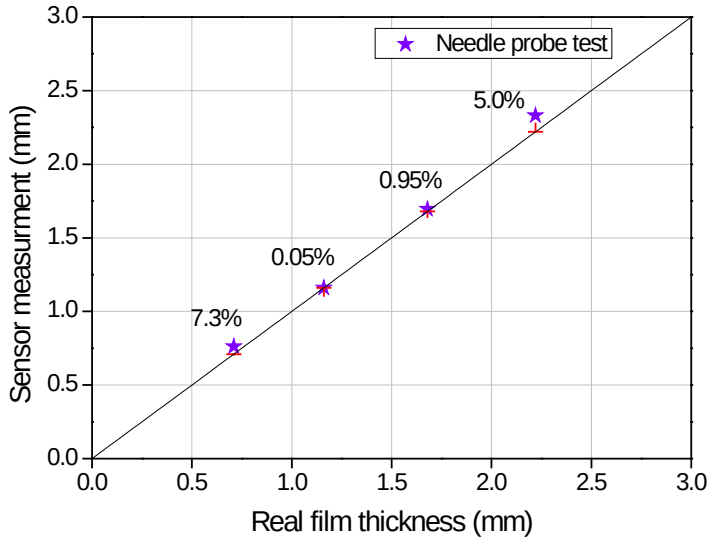

Figure 3.23 Comparison three-ring method with needle probe

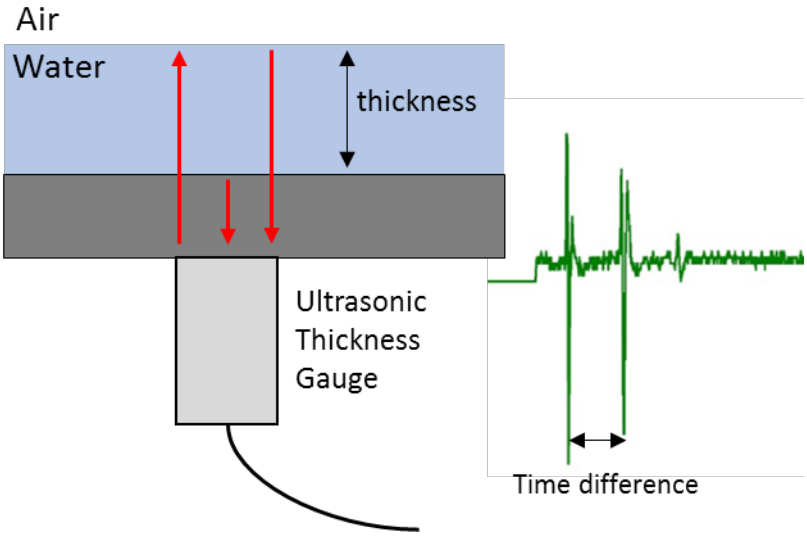

Figure 3.24 Principle of ultrasonic thickness gauge measurement

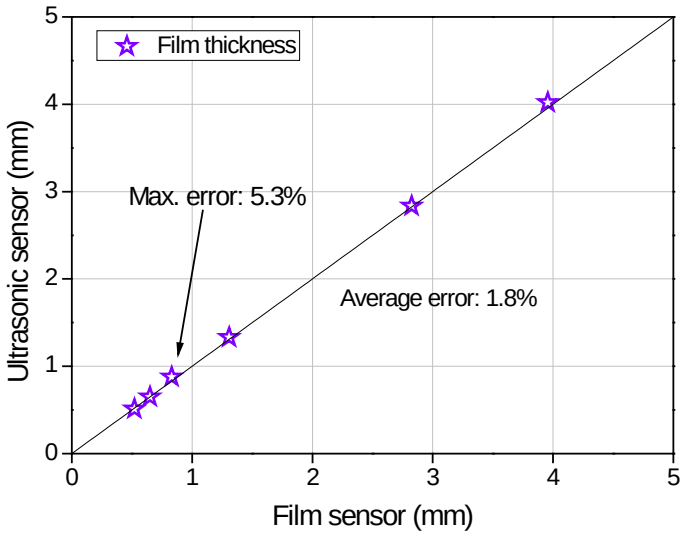

Figure 3.25 Comparison three-ring method with ultrasonic thickness gauge

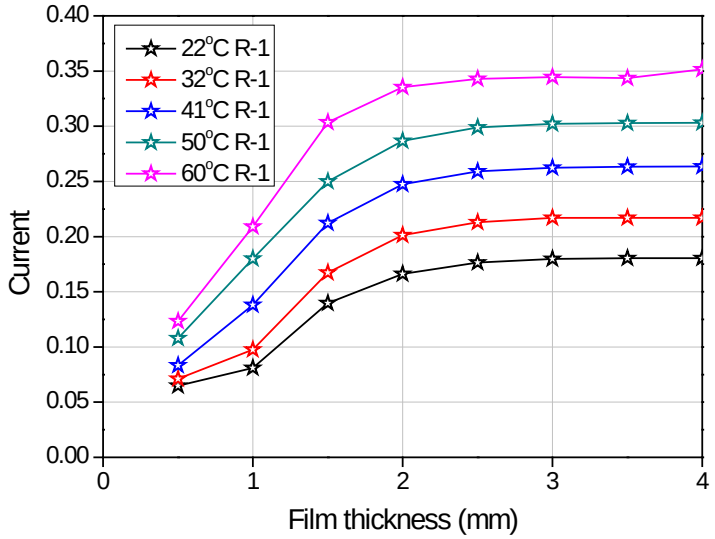

Figure 3.26 Currents flowing to receiver-1 according to temperature

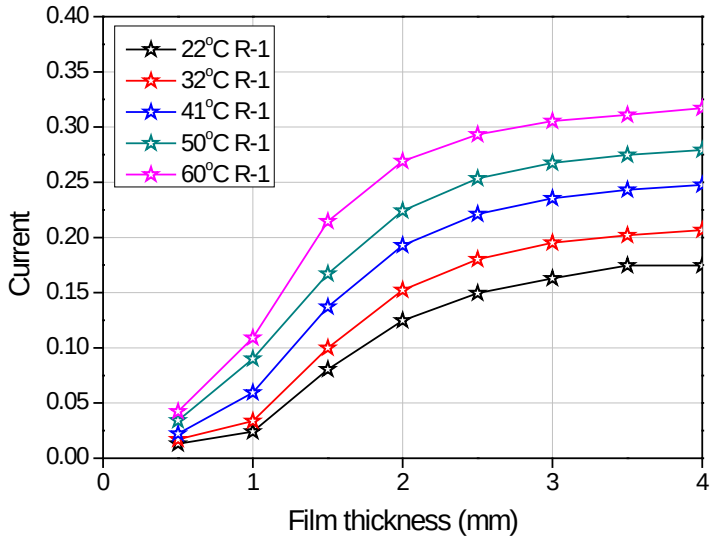

Figure 3.27 Currents flowing to receiver-2 according to temperature

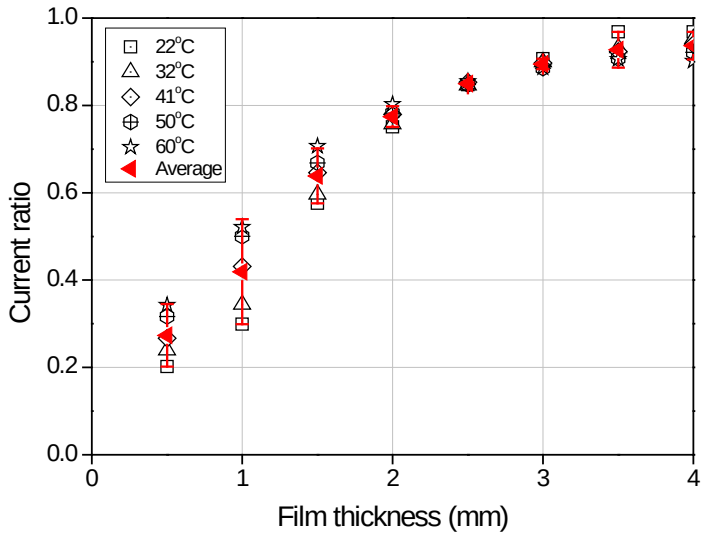

Figure 3.28 Current ratio according to temperature

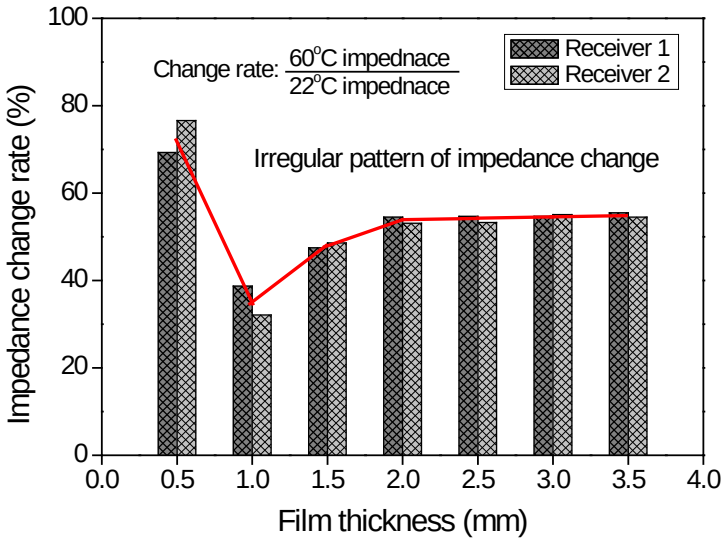

Figure 3.29 Impedance change rate according to film thickness

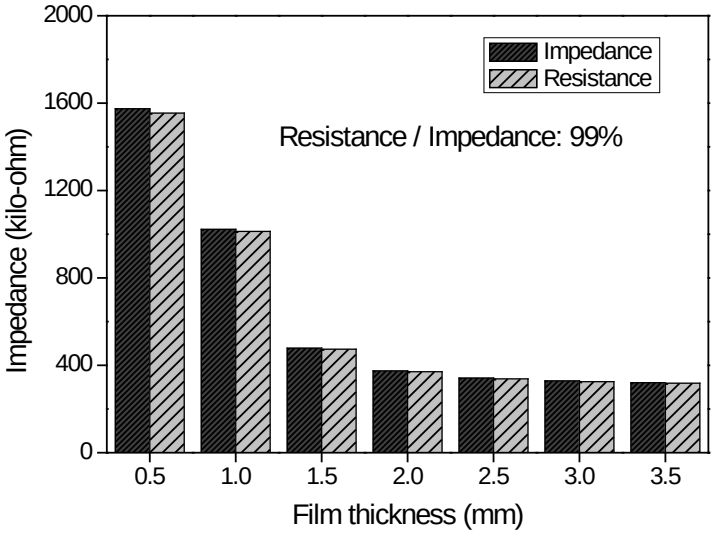

Figure 3.30 Resistance and impedance of the liquid film

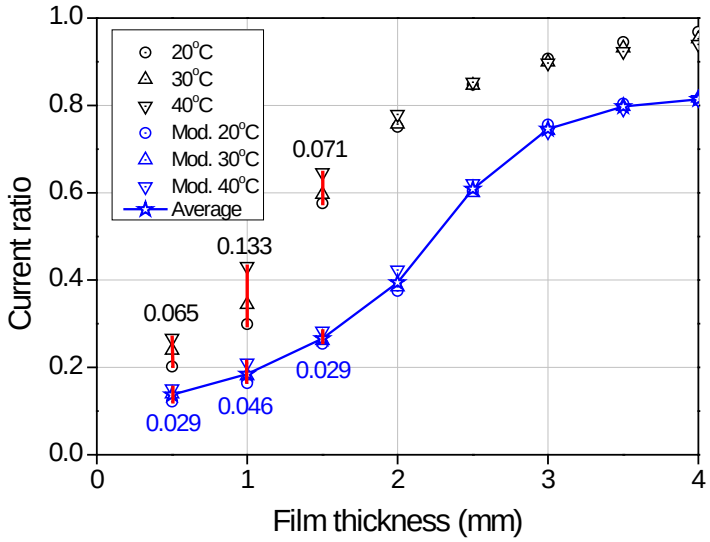

Figure 3.31 Modified current ratio regarding to temperature

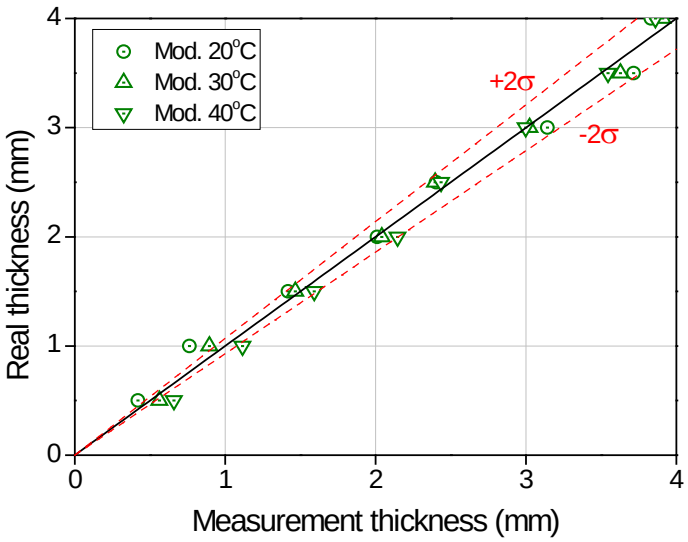

Figure 3.32 Measurement error with using modified current ratio

Chapter 4.

Liquid film flow experiment

4.1 Experimental Setup

Based on the calibration of prototype sensor, a modified FPCB sensor was designed to cover the large area and liquid film flow experiment was performed with the FPCB sensor as shown in Fig. 4.1. The experimental apparatus was designed for the identical flow conditions of two-dimensional film flow conducted by Yang et al. (2015). For simplifying the flow condition, lateral air blowing was not considered. The experimental apparatus is composed with 3 main parts (test section, water storage tank and calibration device). Temperature of the water is controlled at the water tank by heater and cooler. Then the water is injected from nozzle to the FPCB sensor through the pump. Distance from nozzle to FPCB sensor is 25 mm and diameter of the nozzle is 21 mm. Liquid film flow with parabolic shape is developed on the FPCB sensor and flows to the water tank through a drain hole. In the test section, 2 FPCB sensors are installed to measure the area of 360 mm$\times$360 mm width and length. In addition, each FPCB sensor is composed with 24$\times$12 array (total: 288) of ring-type three-ring sensors. Detailed explanation about the FPCB sensor will be discussed in Chapter 4.3. The electrical signals are transmitted through the connecter and cable as shown in Fig. 4.2. The calibration device of this experiment is composed with identical component of calibration

device of prototype sensor. Experimental devices and dimensions of experiment are summarized in Table 4.1, 4.2 and Fig. 4.3 shows the configuration of the experimental apparatus.

4.2 Inducing Channel Transferring System

Total number of probes in FPCB sensor is large (576) for dealing with usual signal transmitting method. In order to manage the signal processing effectively, parallel circuitry which was described in Chapter 3.2 is expanded. Fig. 4.5 shows an overall signal process of the FPCB sensor. 12 transmitter electrodes located in same row are connected in parallel, 24 receiver-1 electrodes and 24 receiver-2 electrodes located in the same column are connected in parallel. Total channel of transmitter line is 24 for each FPCB sensor. The signal lines of receivers are connected to a discrete circuit board. In this discrete circuit board, the current signals are converted to voltage signals and these voltage signals are transmitted to the DAS.

For the measurement of the whole probes in FPCB sensor, the activating channel of the transmitter line should be switched as mentioned in Chapter 3.2. In this study, inducing channel transferring system (switch board) is devised to change the channel of transmitter line. As presented in left side in Fig. 4.5, this switch board changes the channel of transmitter line so that the measurement of liquid film thickness is conducted sequentially. Channel switching can be conducted with manually and automatically. In case of automatic switching, switch board changes the channel by the trigger signal of a function generator. In this experiment, the frequency of trigger signal is confined to 50 Hz because of the performance

limitation in DAQ module. Fig. 4.6. presents a configuration of switch board.

4.3 Modified FPCB Liquid Film Sensor

As described shortly in Chapter 4.1, modified FPCB sensor is manufactured to cover the whole width of falling liquid film. The specific dimensions of electrodes are identical to the prototype sensor. However, additional copper shielding plane is inserted to prevent the cross-talk in this modified FPCB sensor because the cross-talk effect is occurred not only by leakage current but also by electromagnetic induction. Since the ground electrode of prototype sensor only covers the cross-talk from the leakage current, electromagnetic induction should be considered. Fig. 4.7 presents an integrated parallel circuitry system. In this circuitry, magnetic field is developed around I_1. As the I_1 of this FPCB sensor is AC current, the magnetic field changes continuously and the induced currents (I_2 and I_3) are developed consequently. Though induced current I_2 and I_3 are little compared to I_1, the current ratio signal can be distorted. Thus, the electromagnetic induction should be minimized for accurate measurement of current ratio. As mentioned before, copper shielding plane is inserted between the signal lines as shown in Fig. 4.8. The thickness of shielding plane is 30 μm which is identical thickness of circuit line composing the FPCB. With placing the shielding plane, the induced currents decrease compared to the previous prototype sensor. Specific data are compared in Table 4.3.

4.3.1 Calibration with Isothermal Condition

Since every probe composing the FPCB sensor has different characteristics with each other, calibrations for whole probes are demanded for applying it to liquid film flow measurement. However, the size of the modified FPCB sensor is too large to calibrate the whole probes at once. Thus, calibration was conducted with dividing the FPCB sensor into 4 sections.

Calibration range was 0 ~ 3.5 mm with 0.5 mm step and the water condition of the calibration was 18^{o}C and 22 μS/cm. AC 10V, 500 Hz frequency signal is induced to the transmitter lines from the function generator and DAS measures the voltage signal which is converted from current signal. In this calibration, the frequency is lowered to 500 Hz due to the limitation of DAQ performance for detecting the AC signals.

Fig. 4.9. is a plot of typical result of calibration. With increasing the liquid film thickness, the current ratio also becomes larger and saturates at 3.5 mm thickness. Compared to the prototype sensor, the offset point at zero film thickness is rather large. This result is considered as high impedance of FPCB due to the complex and integrated circuit. Even if this result does not affect to measurement significantly, reducing the impedance of circuitry is demanded for improving resolution of the sensor. Fig. 4.10 represents the plot that X-axis is current ratio and Y-axis is film thickness. In this figure, it is found that the resolution of the sensor becomes rather coarse with increasing the film thickness.

For validating the repeatability of this sensor, additional calibration were conducted under the identical experiment condition, and the result is also shown in Fig. 4.9 and 4.10. In the modified FPCB sensor, calibration curve is setup with

applying a spline interpolation method in order to reduce the error by fitting curve and Fig. 4.11 shows the spline interpolation curve based on the calibration result.

As the three-ring method is based on electrical method, the sensor can be affected by electrical noise such as the cross-talk and pump invertor noise. For clarifying the accuracy of the sensor, the measurement error including external noise is analyzed. The error bar is indicated on Fig. 4.12 and the specific error is shown in Table 4.4. This analysis showed that for film thickness up to 1.5 mm, an absolute accuracy of 0.025 mm is achieved and relative average error is 1.6%. For film thickness up to 3.5 mm, the accuracy is reduced to 0.25 mm and relative average error is 4.0%.

4.3.2 Calibration with Temperature Variation

Calibration with various temperature conditions was performed in modified FPCB sensor. Currents flowing to the receivers were measured with increasing the water temperature from 18^{o}C to 38^{o}C. Fig. 4.13 shows that the current ratio is varied with temperature condition which is already measured in the previous prototype sensor. In this modified FPCB sensor, the current ratio decreased with increasing the water temperature which is contrary to result of prototype sensor. By using the normal current ratio, only 10^{o}C range of temperature change is acceptable with around 10% error (see Fig. 4.14 and 4.15). As described in Table 4.5, this result is better than conventional electrical method since the error of electrical method is expected about 15~20%.

The reason of separated current ratio is irregular impedance change as mentioned in Chapter 3.1.3. To extend the varying temperature range, further analysis such as modifying the current ratio form is required to adapt on realistic

experimental condition which has wide range of temperature variation.

4.4 Result of Liquid Film Flow Experiment

As mentioned before, identical water which is used in calibration is required for the accurate measurements because the water condition affects the current ratio. Therefore, liquid film flow experiment was conducted with the same water which was used in calibration. Local film thickness of the liquid film flow developed in the test section was measured by using the calibrated FPCB sensor. Fig. 4.16 shows the test section of the experiment where the film flow is developed. Water is injected from the nozzle and downward liquid film flow is developed with symmetrical parabolic shape. This symmetrical geometry is also measured by Yang et al, (2015).

With controlling the velocity of the water, local film thickness was measured by FPCB sensor. The injection water velocity were 0.48, 0.68, 0.87 m/s (Velocity condition of Yang's experiment was 0.68 m/s). To figure out the time-averaged thickness of the liquid film, measurement for each channel was conducted for 10 seconds. Fig. 4.17 shows the result of 0.48 m/s velocity condition. Left side of the figure is the real liquid film flow which is observed by camera and dotted line is inserted to figure out the trace of the film. Right side of the figure shows the distribution of the local film thickness which is measured by liquid film sensor and the displayed contour is an averaged thickness for 5 seconds. In this figure, the point at (0, 0) is center point of the injecting nozzle.

There were a few features for measuring film thickness in this experiment. Around the boundary of the film, very thin liquid film which does not cover the probe entirely is observed and the currents measured in this section are too little to detect from the electrical noise. Also, the current ratio is out of calibration result.

Thus, the very thin film is excluded in measurement results. As the measurement range of the liquid film sensor is limited to 3.5 mm, the maximum thickness is confined to 3.5 mm in this experiment.

Fig. 4.18 and 4.19 are the results of 0.68 and 0.87 m/s cases. The typical flow pattern is represented in Fig. 4.18. Relatively thick film is distributed around the point (0, 0) since this region is the nearest from the nozzle. As the liquid film flows downward, the width of the liquid film becomes large and the thickness becomes thin. Besides, the hydraulic jump is measured at the boundary of the liquid film. Because of the hydraulic jump, the boundary of the film is thicker than its surroundings. With increasing the injecting velocity (0.48 ~ 0.87 m/s), the width of parabolic shape become large and overall film thickness also become thicker.

Table 4.1. Accuracy of the measurement instruments

Instruments (model)	Span	Accuracy
Thermocouple (K-type)	-200 ~ 1250ºC	±2.2 ºC
Electrical conductance meter (EUTECH Instruments CON450)	0 ~ 200 mS/cm	0.01 μS/cm
Flow meter (Toshiba GF630)	0.0 ~ 10.0 m/s	±0.2 %

Table 4.2 Specific configurations of liquid film flow experiment

Main parts	Components	Specific configurations
Water storage tank	Temperature control system	Cooling with tap water
		Cartridge Heater: 2 kW
Test section	Injection nozzle	Stainless steel pipe Diameter: 21 mm Pipe length for fully developed flow: 640 mm Distance nozzle to FPCB: 25 mm
	FPCB sensor	Width: 180 mm Length: 360 mm
Calibration device	Transfer device	Width: 120 mm Length: 120 mm Resolution: 0.01 mm
	Insulated plane	Width: 200 mm Length: 200 mm Polycarbonate plane

Table 4.3 Cross-talk current reduction by shielding plane

Cross-talk effect	Main receiver (I_1)	Near receiver (I_2)	Far receiver (I_3)
Prototype circuit	-	3.13%	2.36%
Shielding plane circuit	-	0.96%	0.71%

Table 4.4 Measurement error including external noise

Thickness (mm)	Max. absolute error (mm)	Max. relative error (%)	Average error
0.0	-	-	
0.5	0.0097	1.9	
1.0	0.0138	1.4	0.0 ~ 1.5 mm : 1.6%
1.5	0.0228	1.5	
2.0	0.0691	3.5	1.5 ~ 3.5 mm : 4.3%
2.5	0.0875	3.5	
3.0	0.1715	5.7	
3.5	0.2520	7.2	

Table 4.5 Measurement error in 10^{o}C temperature change

Real thickness (mm)	Max. error (%)	Error of conventional electrical method (10^{o}C Variation)
0.6	11	15~20 (%)
0.8	11	
1.0	9	
1.2	9	
1.5	7	
2.0	7	
2.5	8	
3.0	11	

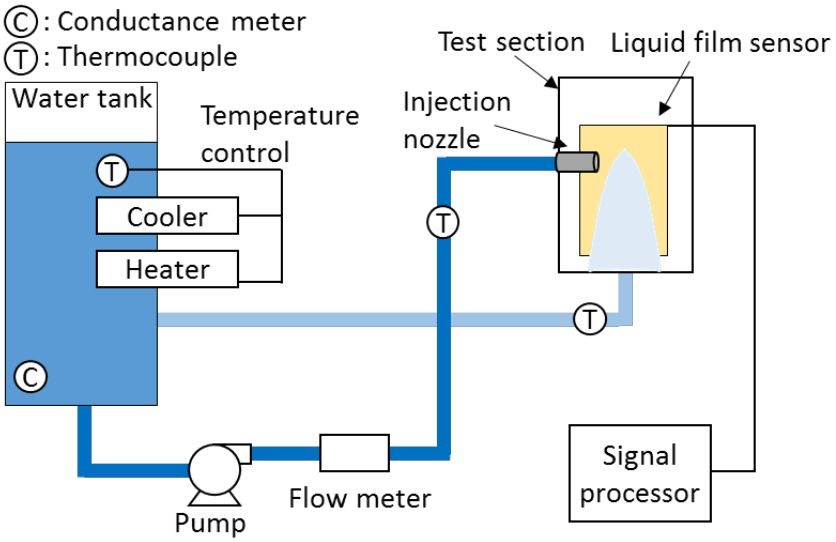

Figure 4.1 Schematic diagram of experimental apparatus

Figure 4.2 Connector and cable of FPCB

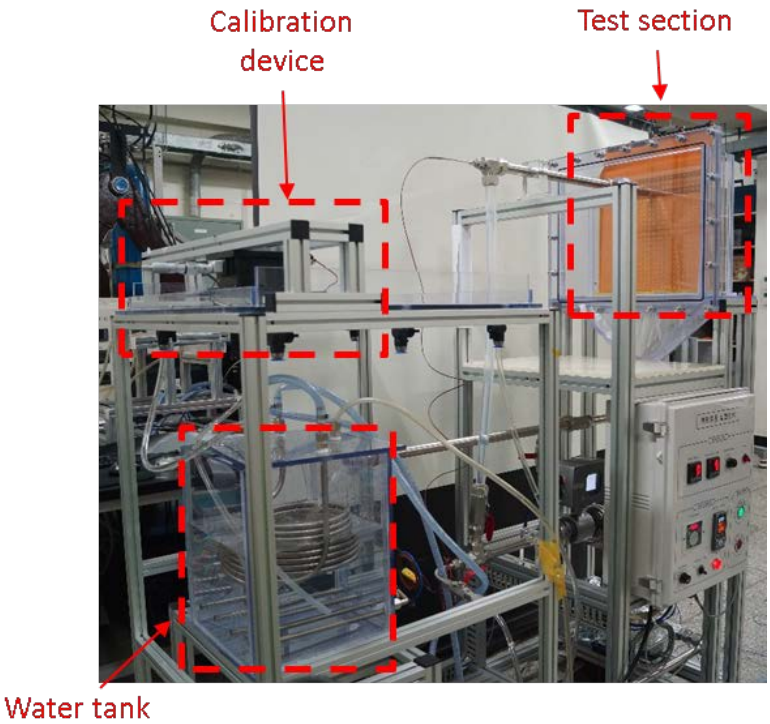

Figure 4.3 Overall configuration of experimental apparatus

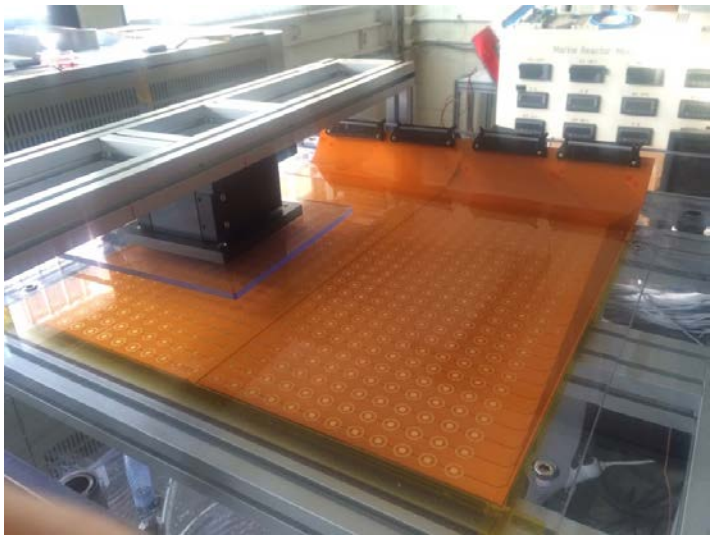

Figure 4.4 Calibration device for modified FPCB sensor

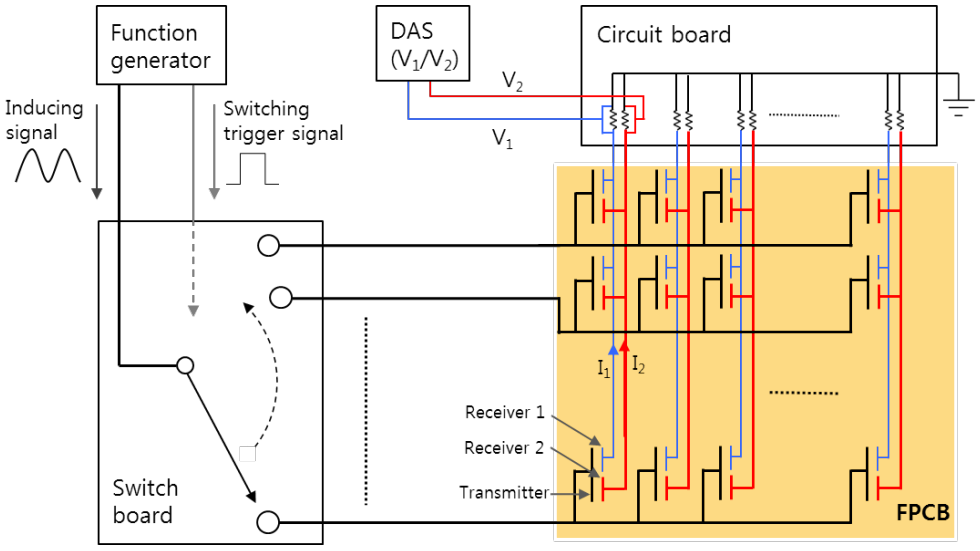

Figure 4.5 Signal transferring process of FPCB

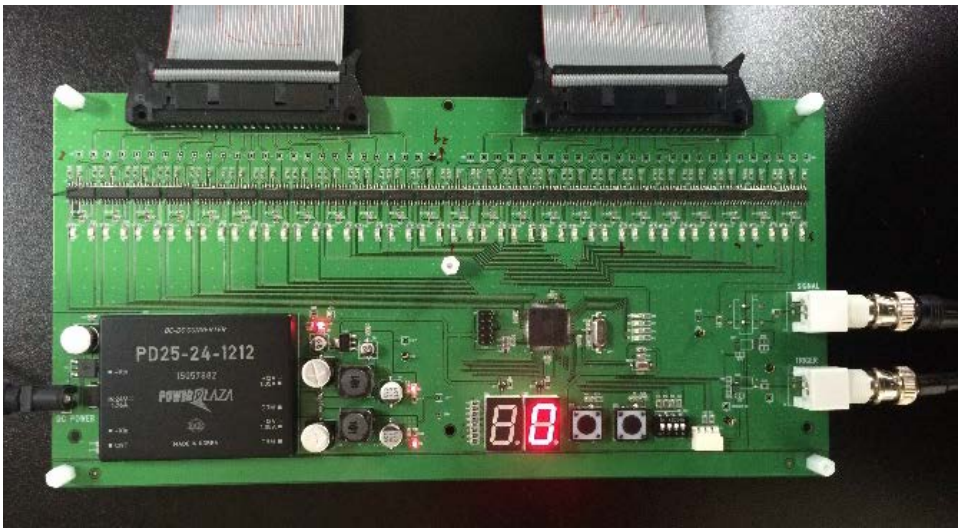

Figure 4.6 Inducing channel transferring system

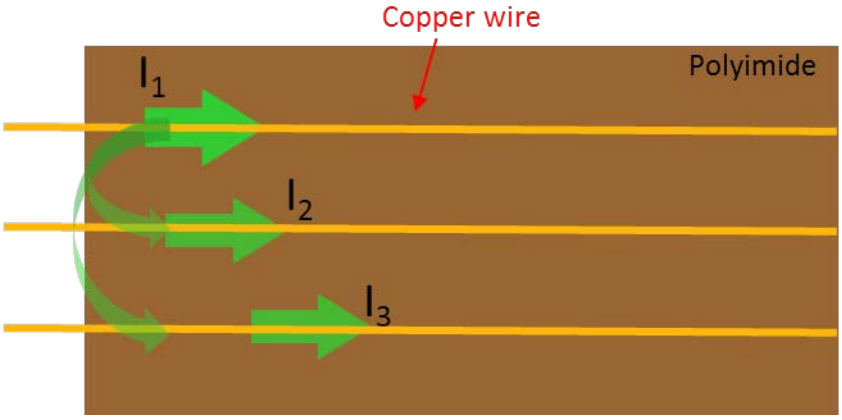

Figure 4.7 Inducing currents in parallel circuit

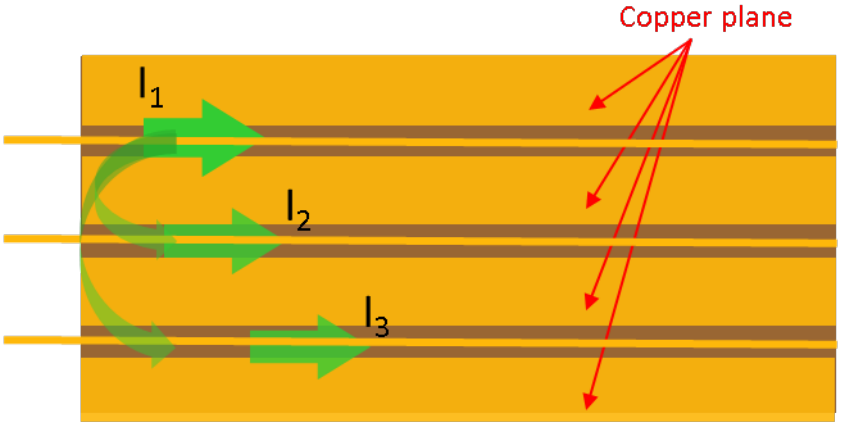

Figure 4.8 Shielding plane arrangement for preventing cross-talk

\

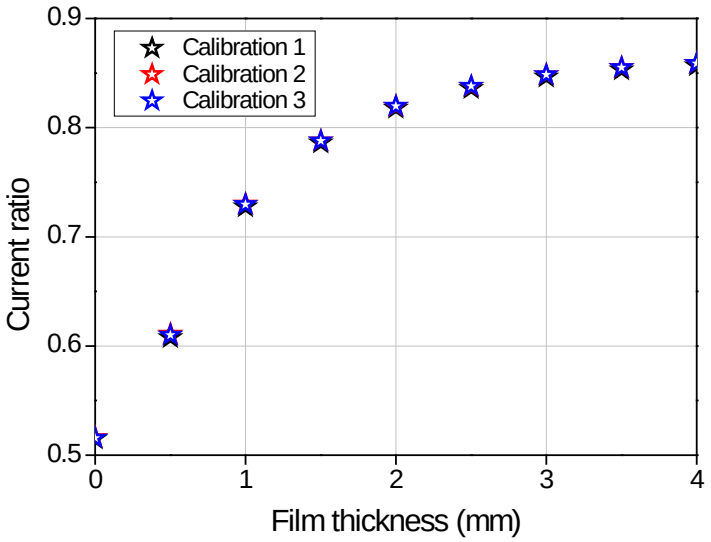

Figure 4.9 Calibration result (X-axis: thickness, Y-axis: current ratio)

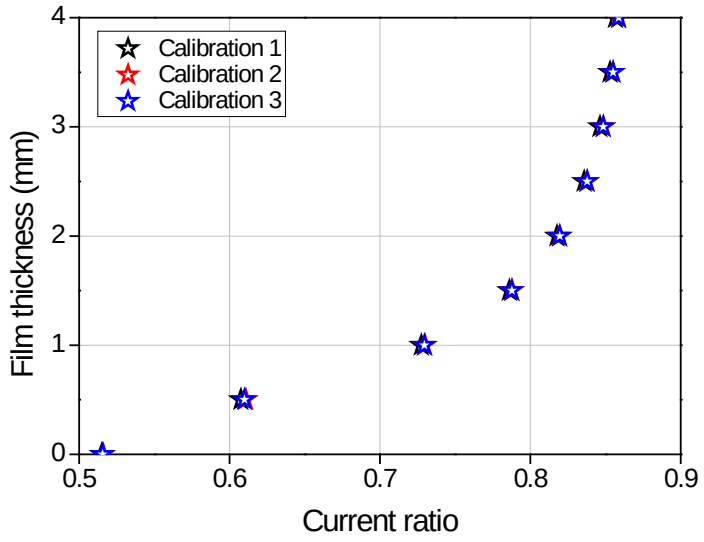

Figure 4.10 Calibration result (X-axis: current ratio, Y-axis: thickness)

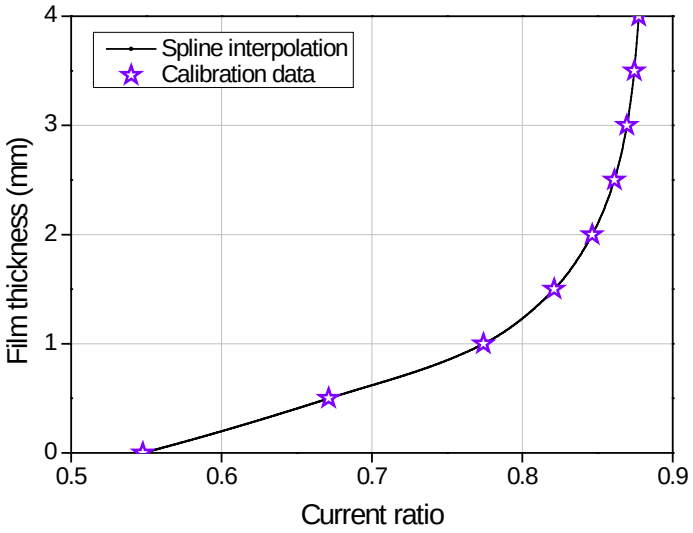

Figure 4.11 Calibration curve (spline interpolation)

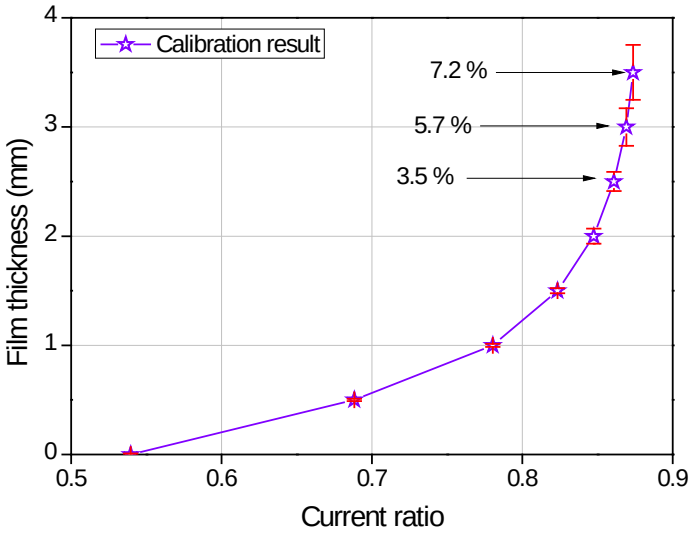

Figure 4.12 Measurement error including external noise

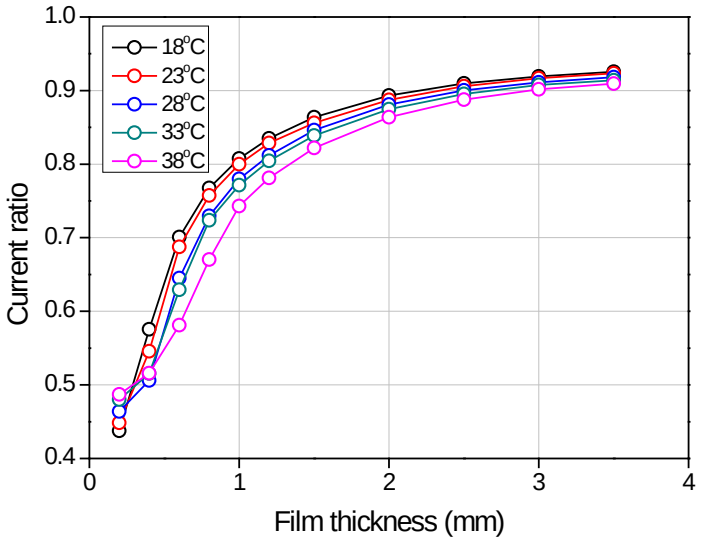

Figure 4.13 Current ratio with temperature change

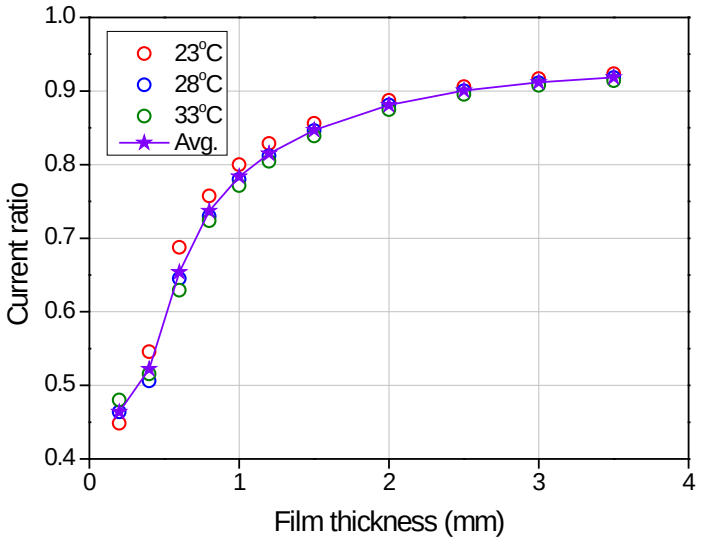

Figure 4.14 Current ratio and averaged data (23 ~ 33°C)

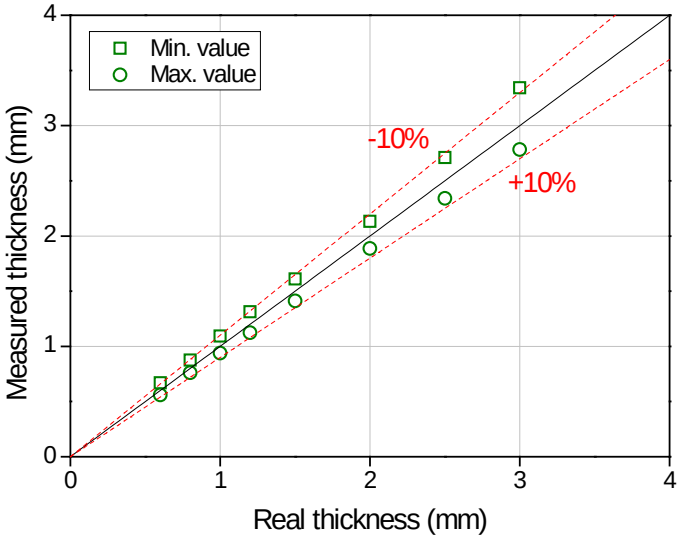

Figure 4.15 Error distribution with 10°C range

Figure 4.16 Test section of liquid film flow experiment

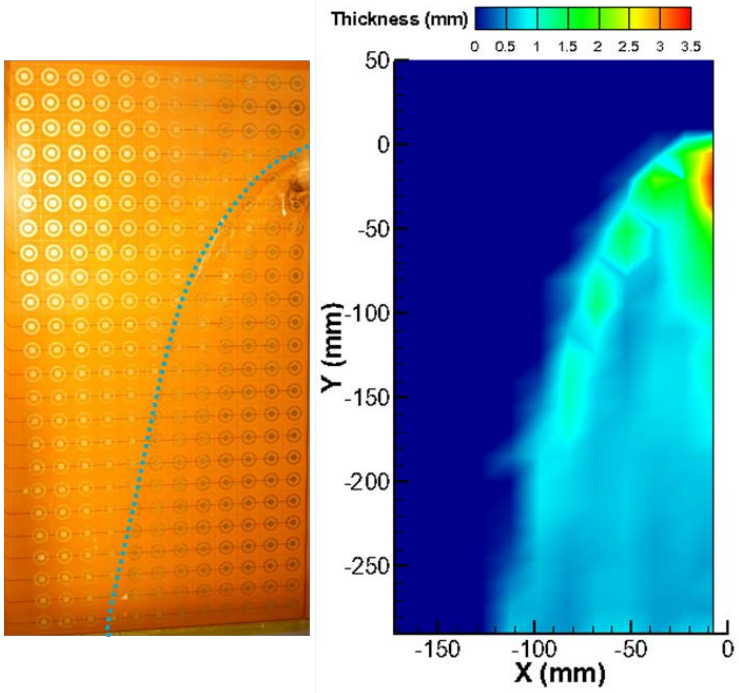

Figure 4.17 Liquid film flow distribution (V_{in}=0.48 m/s)

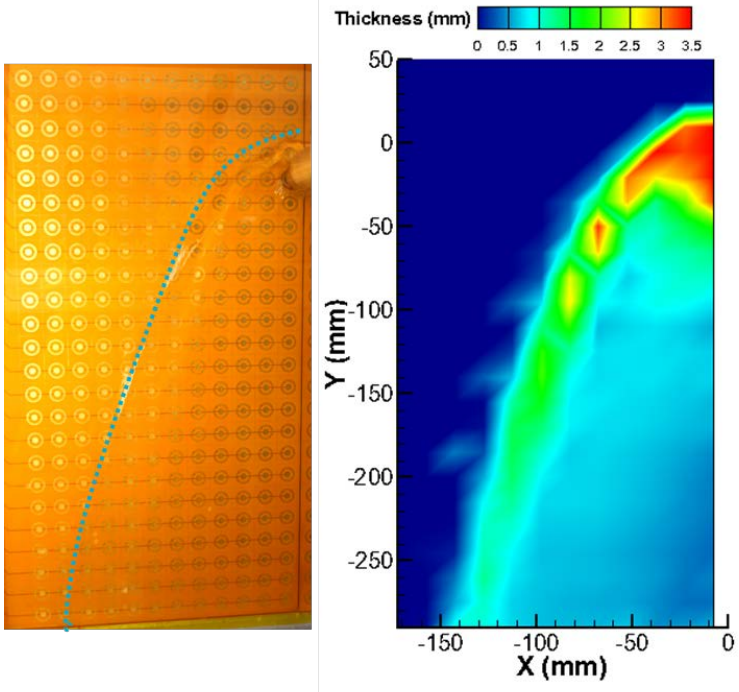

Figure 4.18 Liquid film flow distribution (V_{in}=0.68 m/s)

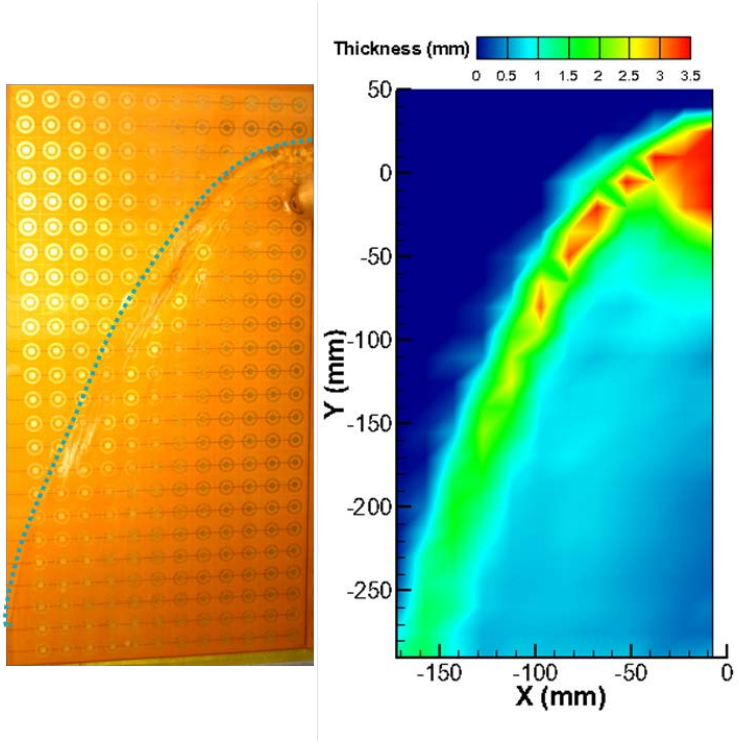

Figure 4.19 Liquid film flow distribution (V_{in}=0.87 m/s)

Chapter 5.

Conclusions

5.1 Summary

In this study, a new type of liquid film sensor was proposed in order to develop the new liquid film sensor which can be used on below conditions.

1. Temperature varying condition which involves the heat transfer
2. High temperature condition for the steam-water flow
3. Curved surface to reflect various geometry condition such as pipe or annular
4. High spatial and time resolution for high precision experiment

Three-ring method and FPCB were coupled to satisfy above conditions. Preliminary experimental study was conducted to confirm the feasibility of coupling the three-ring method with FPCB. Through the preliminary experiment, feasibility was confirmed however limitation of the conventional design was found.

As the conventional design of the three-ring method was not adequate to high precision experiment, design process for electrode geometry was conducted by electrical potential analysis with considering the cross-talk by leakage current. Ring-type electrode design was proposed and a parallel circuitry system for the three-ring method was devised with referring the wire-mesh method. Prototype

FPCB sensor was manufactured to confirm the design result of electrical potential analysis. From the calibration, the performance of the sensor was confirmed. And comparing with other measurement method, the calibration result was validated. The liquid film sensor in this study had 15 mm × 15 mm square spatial resolution and 0.5 ~ 3.5 mm of measurement range. However, the sensor had a confined range of temperature change since the liquid film has irregular impedance change pattern regarding to temperature. To extend the range of temperature change, a modified current ratio was proposed and the range was extended to 20°C.

Based on the prototype sensor, liquid film flow experiment was performed with applying the modified liquid film sensor. The modified liquid film sensor was designed with identical electrode design, but the number of probe was increased to cover the wide range of the liquid film. Besides, copper shielding plane was inserted between the circuits in FPCB to prevent the cross-talk by electromagnetic induction.

For the effective measurement of the FPCB sensor, inducing channel transferring system was developed. By using this inducing channel transferring system, time-averaged local liquid film thickness was measured. In addition, measurement of the whole test section of the FPCB sensor was possible in 1 second with switching the inducing channel automatically.

5.2 Recommendations

The temperature varying range of the ring-type sensor proposed in this study is rather limited. Therefore, further analysis regarding impedance is demanded to extend the temperature varying range. Also, electrode design of the three-ring method can affect to its impedance. Thus, additional experimental study is

suggested for various electrode design.

From the high precision point of view, spatial resolution of the sensor proposed in this study needs to be improved. There was a research adopting periodic boundary to improve the spatial resolution of the liquid film sensor (Damsohn et al., 2009). It is expected that the spatial resolution of the three-ring method also can be enhanced with applying the periodic boundary.

In the present study, the frequency of switching the transmitter channel is too low to measure the film flow instantaneously. However, if the wire-mesh system is applied on this liquid film sensor, the time resolution will increase and the instantaneous measurement will be possible.

FPCB has a lot of strong points that can be applied on thermal-hydraulic experiments. For example, measurement techniques for local temperature, pressure and heat flux are already developed. Thus, with applying the FPCB technology, measuring various physical variables is possible for advanced thermal-hydraulic experiments.

References

M.Damsohn, H. -M. Prasser, Experimental studies of the effect of functional spacers to annular flow in subchannels of a BWR fuel element, Nuclear Engineering and Design, Vol. 240, pp. 3126-3144, 2010

J. H. Yang, H. K. Cho, D. J. Euh, G. C. Park, Experimental study on two-dimensional film flow with local measurement methods, Nuclear Engineering and Design, Vol. 294, pp. 137-151, 2015

Alig, I., H. Oehler, et al, Monitoring of film formation, curing and ageing of coatings by an ultrasonic reflection method, Progress in Organic Coatings 58, pp. 200-208, 2007

Takahama, H. and S. Kato, Longitudinal flow characteristics of vertically falling liquid films without concurrent gas flow, International Journal of Multiphase Flow 6, pp.203-215, 1980

Francesco Paolo D'Aleo, Petros Papadopoulos, H. -M. Prasser, Miniaturized liquid film sensor (MLFS) for two phase flow measurements in square microchannels with high spatial resolution, Flow Measurement and Instrumentation, Vol. 30, pp. 10-17, 2013

M. Hayashi, Temperature-electrical conductivity relation of water for environmental monitoring and geophysical data inversion, Environmental Monitoring and Assessment, pp. 119-128, 2004

H. –M. Prasser, A. Bottger, J. Zschau, A new electrode-mesh tomography for gas-liquid flows, Flow Measurement and Instrumentation, Vol. 9, pp. 111-119, 1998

Coney, M.W.E., 1973, "The theory and application of conductance probes for the measurement of liquid film thickness in two phase flow", Journal of Physics. E: Scientific Instruments, Vol 6, pp.903~910

J. R. Kim, H. K. Cho, D. J. Euh, Experimental study of the characteristics of three flat probe conductance meter, Transactions of the Korean Society of Mechanical Engineers., pp. 378, Dec 2013.

Peter Macleod, A review of flexible circuit technology and its applications, Flexible Circuit Technology, 2002

E. Pritchard, M. Mahfouz, B. Evans III, S. Eliza, M. Haider, 2008, Flexible capacitive sensors for high resolution pressure measurement, IEEE Sensors 2008 conference

M. Shikida, K. Yoshikawa, S. Iwai, K. Sato, 2012, Flexible flow sensor for large-scale air-conditioning network system, Sensors and Actuators A: Physical 188, pp 2-8

Daniel J. Lichtenwalner, Aaron E. Hydrick, Angus I. Kingon, 2007, Flexible thin film temperature and starin sensor array utilizing a novel sensing concept, Sensors and Actuators A 135, pp 593-597

Takahiro Arai, Masahiro Furuya, Taizo Kanai, Kenetsu Shirakawa, Concurrent upward liquid slug dynamics on both surfaces of annular channel acquired with liquid film sensor, Experimental Thermal and Fluid Science, Vol. 60, pp. 337-345, 2015

COMSOL Multiphysics User’s Guide, Ver. 5.1 , 2015COMSOL

G. Vasilescu, Electronic Noise and Interfering Signals Principles and Applications,

Springer, 1999

M.Damsohn, H. -M. Prasser, High-speed liquid sensor for two-phase flows with high spatial resolution based on electrical conductance, Flow Measurement and Instrumentation, Vol.20, pp.1-14, 2009

LabVIEW 2009, National Instruments, 2009

Appendix A

Signal Output of Uneven Film Thickness Condition

Generally, liquid film covering the electrode of FPCB sensor does not maintain flat plane surface. As the principle of the three-ring method is based on the Ohm's law, it is expected that the signal output of uneven liquid film will be coincide with that of flat film which has equal mean thickness. However, the electrical potential analysis and calibration were conducted with assuming that the liquid film is ideally even plane shape. Therefore, it is required to confirm the signal output of the sensor in case of the liquid film with uneven surface.

In order to confirm the above issue, additional electrical potential analysis was conducted under the calculation domain as shown in Fig. A.1. Calculation domain is composed with liquid film, electrodes, insulated boundary similar with that of Chapter 3.1. For representing the uneven liquid film, trapezoidal geometry was determined as a shape of liquid film. The trapezoidal geometry has uneven top plane but the mean height of both sides is identical to the central height of the film. With increasing the basis thickness of the film, current ratio was calculated. The calculation was also conducted with changing the inclination of the trapezoid (α: 0.2 ~ 1.0 mm) Result of calculation is presented in Fig. A. 2. The current ratio output of trapezoidal geometry is identical to that of the flat plane condition which has an equal average height.

In conclusion, the signal output of the uneven liquid film can be considered as that of flat liquid film composed of same mean height.

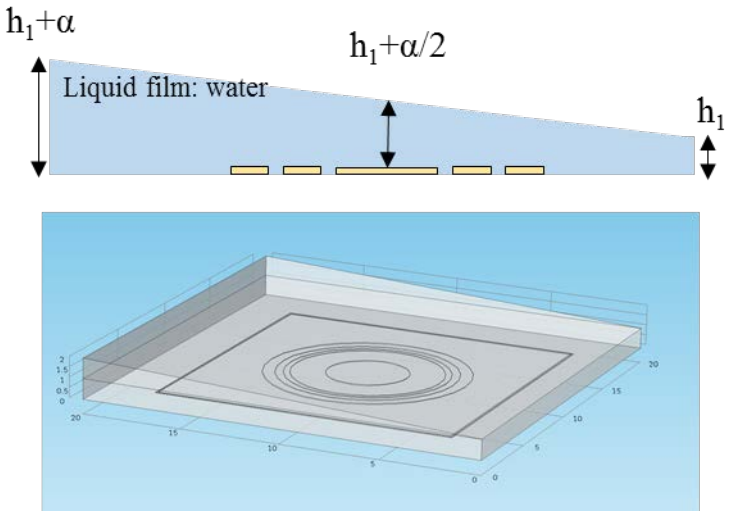

Figure A.1 Electrical potential calculation domain for uneven liquid film

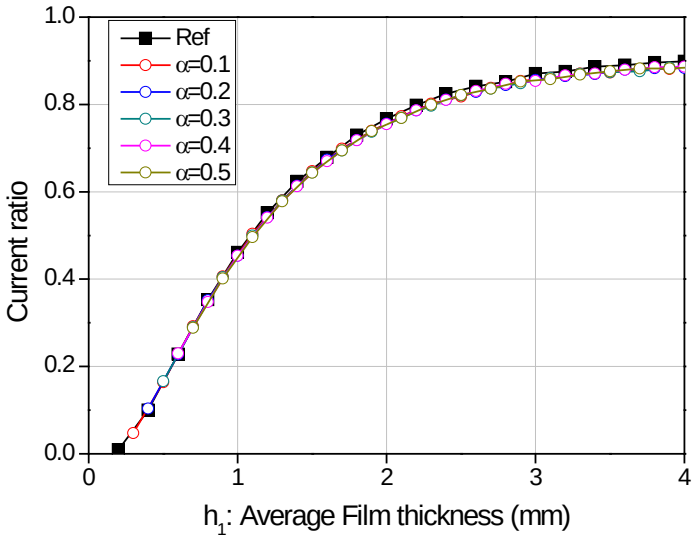

Figure A.2 Calculation result of current ratio under uneven film

Appendix B

Uncertainty Propagation of Averaged Liquid Film Thickness

The uncertainty of the averaged liquid film thickness (T_m) can be estimated by error propagation method. In case of the averaged value produced by N numbers of data (T_i), the error of the averaged value (e_m) can be expressed as Eq. (B.1).

$$e_m = \sqrt{\frac{\sum_{i=1}^{N} {e_i}^2}{N}} \tag{B.1}$$

Where, e_i is an error of the each measurement value and this can be calculated as Eq. (B.2) since the error of the liquid film sensor is 4%.

$$e_i = 0.04 \times T_i \tag{B.2}$$

The liquid film thickness of liquid film flow experiment is averaged value of 500 data. Thus, averaged error is calculated with square root of 500 errors. Fig. B.1 shows the averaged local uncertainty and film thickness. Since the measurement result is two-dimensional data, the uncertainty of the whole local point is presented by using contour graph. The uncertainty of most points are below than 5%. However, the uncertainty of film edge region was relatively high because the varying range of film thickness is rather broad. Similar pattern is also found in standard deviation of the film thickness as presented in Fig. B.2.

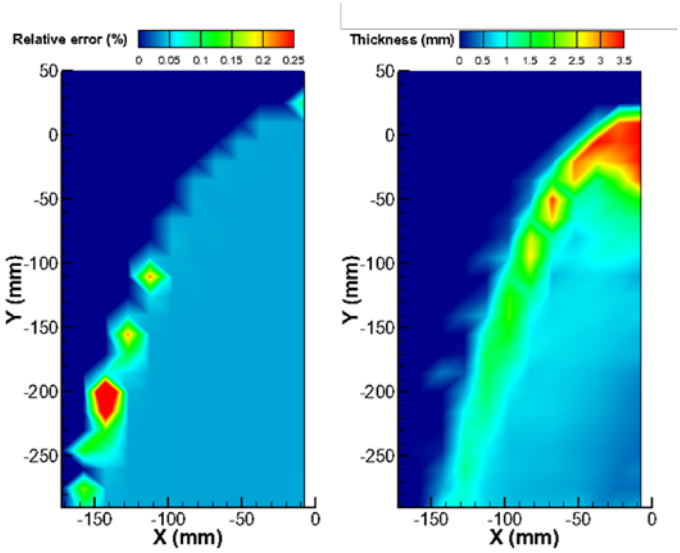

Figure B.1 Contour of relative measurement error and averaged film thickness

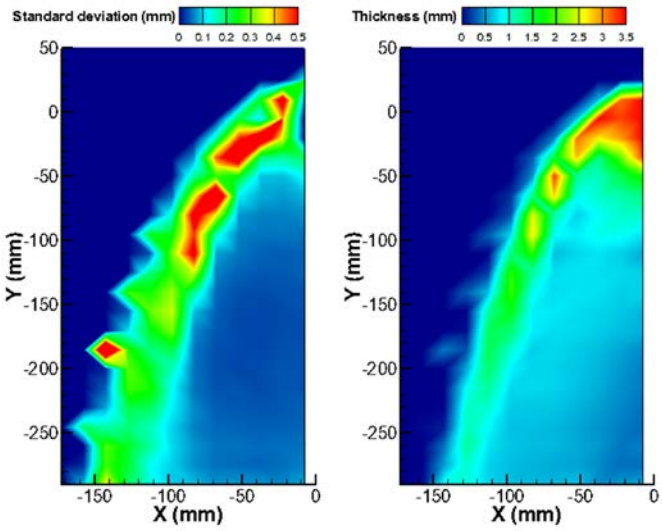

Figure B.2 Contour of standard deviation and averaged film thickness

요약 (국문초록)

최근 원자력 안전 분야에서는 고정밀 2상 유동 실험에 대한 관심이 많아지면서 원자로 내에서 발생하는 액막 유동 또는 환형 유동과 같은 2상 유동에 대한 실험들이 진행되고 있다. 액막의 두께는 2상 유동 현상 연구에 있어 중요한 요소 중 하나이기에, 2상 유동 조건에서 액막의 두께를 측정하기 위한 기법에 대한 다양한 연구들이 진행되어 왔다. 하지만 기존의 일반적인 액막 두께 측정 방식으로는 원자력 발전소에서 주로 나타나는 2상 유동 조건에서 고정밀성을 갖춘 측정을 하기 어려웠다. 최근 전기적 기법을 인쇄회로기판(PCB) 혹은 연성회로기판(FPCB)에 적용시키고, 이를 Wire-mesh (Prasser et al., 1998) 회로와 연동하는 방법을 통해서 시간 및 공간에 대한 고정밀성을 동시에 만족시키는 측정 기법이 개발되었다. 이러한 측정 기법이 개발된 이후 다양한 유로 형상에서 2상 유동 실험이 진행되었다. 하지만, 일반적인 전기적 방법을 적용한 액막 센서는 유체의 온도에 의한 전기 전도도 변화로 열전달이 수반되는 유동 조건에서는 적용할 수 없고, 이런 제한으로 인해 매우 한정적인 조건에서만 실험이 되었다. 원자력 발전소에서 나타나는 대부분의 2상 유동현상은 열전달을 포함하고 있기 때문에 유체의 온도가 국부적으로 변하고 상변화 현상이 나타난다. 따라서 정확한 2상 유동 분석을 위해서는 변온 조건에서 실험이 진행되어야 한다.

본 연구는 3-전극 기법을 도입해서 유체의 온도가 변하는 조건에서도 액막 두께를 측정할 수 있는 액막 센서를 개발하는 것을 목표로 두었다. 이러한 목표를 위해 전기장 해석을 통해서 액막 유동 실험에 적합한 3-전극 센서의 전극을 설계하는 과정을 거쳤다. 또한 센서의 전극을 FPCB에 제작하는 방식을 통해서 고온 및 곡면의 실험 조건에도 적용할 수 있는 센서를 개발했으며, 시

제품 제작을 통해서 액막 센서로서의 가능성을 확인했다. 시제품 센서에 대한 시험 결과를 기반으로 넓은 면적에서 액막 두께를 측정할 수 있도록 FPCB 센서를 확장 설계 및 제작했으며, 액막 센서를 활용한 기초적인 액막 유동 실험을 수행했다. 한편, 교정 과정을 통해서 기존의 3-전극 이론에서 제안된 전류비를 통한 온도 보상이 한정된 온도 범위에서만 가능한 것을 확인했으며, 센서의 온도 보상 범위를 확장시키기 위해 수정된 전류비 형태를 제안했다.

주요어: 액막 두께, 액막 두께 센서, 3-전극 기법, 연성회로기판(FPCB), 2상 유동 실험

학번: 2014-21423